Thesis for the Degree of Master of Science

The Calibration System for IGRINS, a High Resolution Near-IR Spectrograph

Heeyoung Oh

School of Space Research
Graduate School
Kyung Hee University
Seoul, Korea

August, 2010

The Calibration System for IGRINS, a High Resolution Near-IR Spectrograph

Heeyoung Oh

School of Space Research
Graduate School
Kyung Hee University
Seoul, Korea

August, 2010

The Calibration System for IGRINS,
a High Resolution Near-IR Spectrograph

by

Heeyoung Oh

advised by

Dr. Soojong Pak

Submitted to the School of Space Science
and Faculty of the Graduate School of Kyung Hee University
in partial fulfillment of the requirement for degree of
Master of Science

Dissertation Committee

....
Dr. Soojong Pak

....
Dr. In-Soo Yuk

....
Dr. Ho Jin

The Calibration System for IGRINS, a High Resolution Near-IR Spectrograph

ABSTRACT

We present development of the calibration system for IGRINS (the Immersion GRating INfrared Spectrograph). IGRINS is a high resolution infrared spectrograph which is developed by a collaboration of the University of Texas at Austin, Korea Astronomy and Space Science Institute, and Kyung Hee University. IGRINS is the forerunner for GMTNIRS (the Giant Magellan Telescope Near Infrared Spectrograph) which has been selected for study of GMT first-light instruments. IGRINS uses a silicon immersion grating as an echelle grating and it has a resolving power of 40,000 in *H*- (1.49μm -1.80μm) and *K*- (1.96 μm -2.46 μm) bandpass.

To establish the calibration concept of our high resolution instrument, we reviewed a few existing similar spectrographs, e.g., BOES, CRIRES, and IRCS. There are two main purposes for the calibration. Those are: 1) to get a distortion solution and a wavelength solution using line reference sources; 2) to correct pixel-to-pixel sensitivity variations by flat frames. For the IGRINS wavelength calibration, we can use hallow cathode lamps to get the reference lines. The telluric OH emission lines and the telluric absorption lines can be other reference sources. We investigated the advantages and disadvantages of each calibration sources. For flat-fielding, we will use a tungsten halogen lamp with an integrating sphere to get blackbody radiations. For selecting an appropriate line lamp, we count the number of available lines per each order based on the acceptable dynamic range of the line intensity. For our *H*- and *K*- band application, we confirmed that the uranium lamp is the most preferable.

We designed calibration optics with Code V and conducted its performance analysis using LightTools software package. We designed lens barrels and a conceptual calibration box containing the integrating sphere, the line lamp, folding mirrors and moving parts. We organized the moving positions of calibration hardware considering the observing scenarios.

Table of Contents

Abstract ……………………………………………………………………………… i

List of Figures……………………………………………………………………………..iv

List of Tables…………………………………………………………………………………vi

1. INTRODUCTION …………………………………………………………………………..1

1.1 Spectrograph…………………………………………………………………………1

1.2 IGRINS…………………………………………………………………………………2

1.3 Calibration Purpose and Methods…………………………………………………..8

1.4 Purpose of This Work ……………………………………………………………….9

2. CALIBRATION CONCEPT FOR IGRINS…………………………………………..10

2.1 Calibration System Structure………………………………………………………10

2.2 Calibration Sequence…………………………………………………………………13

2.2.1 Pre-Processing and Flat……………………………………………………….13

2.2.2 Line Lamp………………………………………………………………………..13

2.2.3 Standard Star…………………………………………………………………….14

3. WAVELENGTH CALIBRATION ………………………………………………………15

3.1 Echellogram……………………………………………………………………………16

3.2 Source Selection………………………………………………………………………19

3.2.1 Telluric Absorption Lines……………………………………………………….19

3.2.2 Telluric OH Emission Lines……….…………………..…………………20

3.2.3 Th-Ar Lamp…………………………………………………...………….25

3.2.4 Uranium Lamp………………………………………………………………25

3.2.5 Number of Lines and Choice of Lamp………………..…………………26

4. FLAT SOURCE ……………………………..………….…………………44

5. OPTO-MECHANICAL DESIGN ………………………………..…………..…..46

5.1 Optical Design……………………………..…….……………………46

5.1.1 Concept…………………………..……..…..……………………..46

5.1.2 Requirement………………………………..………………………47

5.1.3 Optics Design and Performance……………..……...………..……..…51

5.2 Lens Barrel …………..…………………………………..………………55

5.3 Calibration Box Design………………….….…………….……………………59

5.4 Observing Mode and Moving Part ………..……………………………………61

6. SUMMARY AND FUTURE WORK ……………..……………………………66

REFERENCES……………………………………………………….……………68

List of Figures

Figure 1. – Conceptual design of the cold optics in IGRINS dewar ………………….……..…....5

Figure 2. – Silicon immersion grating…………………………………………….……..………6

Figure 3. – IGRINS optics design (Yuk et al. 2010)……………………………………………7

Figure 4. – Conceptual arrangement of IGRINS calibration sources …………………….……11

Figure 5. – Optical layout of calibration sources……………………………………..……...12

Figure 6. – IGRINS dada reduction process……………………………………………….15

Figure 7. – IGRINS *H*- band echellogram…………………………………………………17

Figure 8. – IGRINS *K*- band echellogram………………………..……………………..…18

Figure 9. – Source line allocation in IGRINS wave bands ……………………………………..21

Figure 10. – Telluric features at *H*- and *K*- band (Seo et al. 2010)……………….……………..22

Figure 11. – Various OH molecule transition processes caused by rotation – vibration band (Rousselot et al. 2000) in infrared …………………………………………...23

Figure 12. – OH band features appeared in *H*- and *K*- band wavelength (Rousselot et al. 2000)……………………………………………………………………….24

Figure 13. – Number of Th-Ar lines in *H*- and *K*- band…………………….………….27

Figure 14. – Number of OH emission lines in *H*- and *K*- band……………………………….28

Figure 15. – Number of uranium lines in *K*- band…………………………………………….29

Figure 16. – Histogram shows number of lines at each IGRINS *H*- and *K*- band order…….43

Figure 17. – The performance of integrating sphere and gold-coated integrating sphere….…44

Figure 18. – An optical design of Subaru Nasmyth calibration unit (top) and BOES calibration optics…………………………………………………………………………49

Figure 19. – Space estimation for calibration optics……………………………………………..50

Figure 20. – IGRINS calibration optics design layout………………………………………...52

Figure 21. – Flatness error of photon flux at focal plane……………………………………...54

Figure 22. – Calibration optics lens barrel……………………………………………………….57

Figure 23. – Composition of barrel 1(left) and barrel 2(right) ……………………………….58

Figure 24. – Conceptual model of calibration box ……………..………..………………...…60

Figure 25. – IGRINS observing Scenario………………………………………………………..63

Figure 26. – 4 different positions of calibration moving parts…………………..….…………..65

List of Tables

Table 1. – IGRINS design parameters (Yuk et al. 2010)……………………………………4

Table 2. – Th-Ar lines in *H*- Band (Kerber et al. 2008)……………….……………........……30

Table 3. – Th-Ar lines in *K*- Band (Kerber et al. 2008)……………….…………….…..………33

Table 4. – OH lines in *H*- Band (Rousselot et al. 2000)...……………………………….…...…35

Table 5. – OH lines in *K*- Band (Rousselot et al. 2000)……...………...………………..…...…38

Table 6. – U lines in *K*- Band (Conway et al. 1984).....…………………………..….…....…40

Table 7. – Calibration optics parameters……………………………………...……..…….53

Table 8. – Position of moving mirrors in IGRINS calibration box……………………......….64

1. INTRODUCTION

1.1 Spectrograph

The word spectrum was introduced into optics in 17^{th} century, by observation of dispersed light colors of white light through a prism. Spectrum referred to a plot of light intensity or power as a function of wavelength or frequency. The first astronomical spectroscopic observation was Isaac Newton's solar observation in 1666. Joseph von Fraunhofer first described the dark bands appeared in solar spectrum in 1814. After this, the astronomical spectroscopy has begun in earnest.

A spectrograph (spectrometer or spectroscope) is an instrument which can measure the properties of light over the electromagnetic spectrum. In astronomy, the spectroscopy has been used to derive physical properties of planets, stars, interstellar medium, and galaxies, etc.

We can classify the spectrographs into several types (Birney et al. 2006) according to its principles of operation. Prism spectrograph uses the indexes of refractions of light that varies along the wavelength. Since prisms are simple and have high throughput, early experimenters such like Newton, Huggins, Secchi used prism spectrographs. The prisms, however, not commonly used today. Gratings are based on the properties of diffraction and interference of light. The incident light through a slit is being dispersed by reflecting (or transmitting) on the surface of diffraction gratings which have series of grooves. There are two spectrograph using interference. A Fourier Transform Spectrometer (FTS) uses the principle of Michelson interferometer. The FTS contains a fixed beam splitter, movable mirrors and the phase difference between two mirrors produce the interference effect (Pak 2007). A Fabry-Perot Spectrometer (FPS) uses multi-beam interference (Pak 2000) with two highly reflecting parallel mirrors.

Echelles are terms which refer to the particular gratings. Echelle has small number of grooves relatively and very large blaze angle (e.g., 79 grooves per millimeter and blaze angle of 63.5°). They are used in very high orders (e.g., order number m = 100) where they can perform the high dispersion and they have been used in fields of astronomical spectroscopy which requires high dispersion and resolving power (e.g., R ~ 40,000). Overlapping of diffraction orders is one problem arisen by using higher orders and we can solve this problem by placing a cross – disperser between the echelle grating and a camera. Ordinary gratings or prisms are used as cross – disperser and this should be mounted perpendicularly to the echelle grating. Echelles usually specified by its groove number per millimeter and its R number. R number equals tangent of the blaze angle, i.e., R2 echelle has a blaze angle about 63.1˚ and R5 has near 78.7˚.

Infrared (the electromagnetic radiation between 0.7 and 350 μm; Glass 1999) spectrograph has been developed due to the growth of infrared detector (e.g., InAs, InSb, HgCdTe) technology. There are dozens of infrared spectrograph in the world and several examples are MOSFIRE (Multi-Object Spectrometer for Infra-Red Exploration; McLean et al. 2008) for Keck observatory, CRIRES (CRyogenic InfraRed Echelle Spectrograph; Kaufl et al. 2004) for VLT of European Southern Ovservatory, SpeX (Rayner et al. 2003) for NASA Infrared Telescope Facility (IRTF). The spectrographs for the space telescopes have also developed. ISO (the Infrared Space Observatory) is the first mission which uses true infrared array, and it contains SWS (Short-Wavelength Spectrometer) and LWS (long-Wavelength Spectrometer). IRS (the Infrared Spectrograph; Houck et al. 2004) for Spitzer space telescope, NIRSpec (Near Infrared Spectrograph; Jakosen et al. 2010) for the James Webb Space Telescope and HIFI (Heterodyne Instrument for the Far-Infrared; de Graauw et al. 1998, 2008) on the Herschel Space Observatory are more examples.

1.2 IGRINS

IGRINS (the Immersion GRating INfrared Spectrograph) is a high resolution infrared spectrograph which is developed by a collaboration of the University of Texas at Austin, Korea Astronomy and Space Science Institute, and Kyung Hee University (Yuk et al. 2010). IGRINS is the forerunner for GMTNIRS (the Giant Magellan Telescope Near Infrared Spectrograph; Jaffe et al. 2006) which has been selected for study of GMT first-light instruments. IGRINS uses a silicon immersion grating (Jaffe et al. 2008) as an echelle grating and VPH gratings as cross dispersers. Due to the property of silicon (refractive index n = 3.4), the immersion instrument can have very small collimated beam diameter while having high resolving power. Thus, the size of IGRINS optical bench (Figure 1) is significantly compact compared with an instrument using typical diffraction grating. Figure 2 show the appearance of silicon immersion grating manufactured by University of Texas at Austin. Additionally, dichroic mirror divides the beam into two paths of *H*- and *K*- band camera therefore IGRINS can observe the whole *H*- and *K*- bands in a single exposure.

In Table 1, we list the IGRINS design parameters. IGRINS will have a resolving power of 40,000 with 0.68" and 1.00" entrance slit width at 4m and 2.7m telescopes, respectively (Yuk et al. 2010). Two HAWAII 2RG detectors will be used for *H*- (1.49μm -1.80μm) and *K*- (1.96 μm -2.46 μm) band cameras (Figure 3). IGRINS will be placed initially on the McDonald 2.7m Harlan J. Smith telescope and later on 4-8m class telescopes.

Table 1

IGRINS design parameters (Yuk et al. 2010).

Item		*H*-band	*K*-band
Wavelength [μm], band center (range)		1.65 (1.49 - 1.8)	2.16 (1.96 - 2.46)
Slit [arcsec] (Width × Length)	4m telescope	0.68 × 10	
	2.7m telescope	1.00 ×14.7	
Resolving Power, R		40,000	
Beam size [mm]		25	
Main dispersion grating (Immersion grating)	Glass material	Silicon	
	Grating angle [deg]	71.56 (R3)	
	Line density [l/mm]	36.5	
	Orders (min-max)	98 - 122	72 - 92
Cross dispersion grating (VPHG, first order)	Glass material	Fused silica	
	Grating angle [deg]	32.4	26.1
	Line density [l/mm]	650	400
	Order separation [arcsec] (min-max)	11.8 - 18.3	12.1 - 20.2
Detector		HAWAII-2RG	HAWAII-2RG

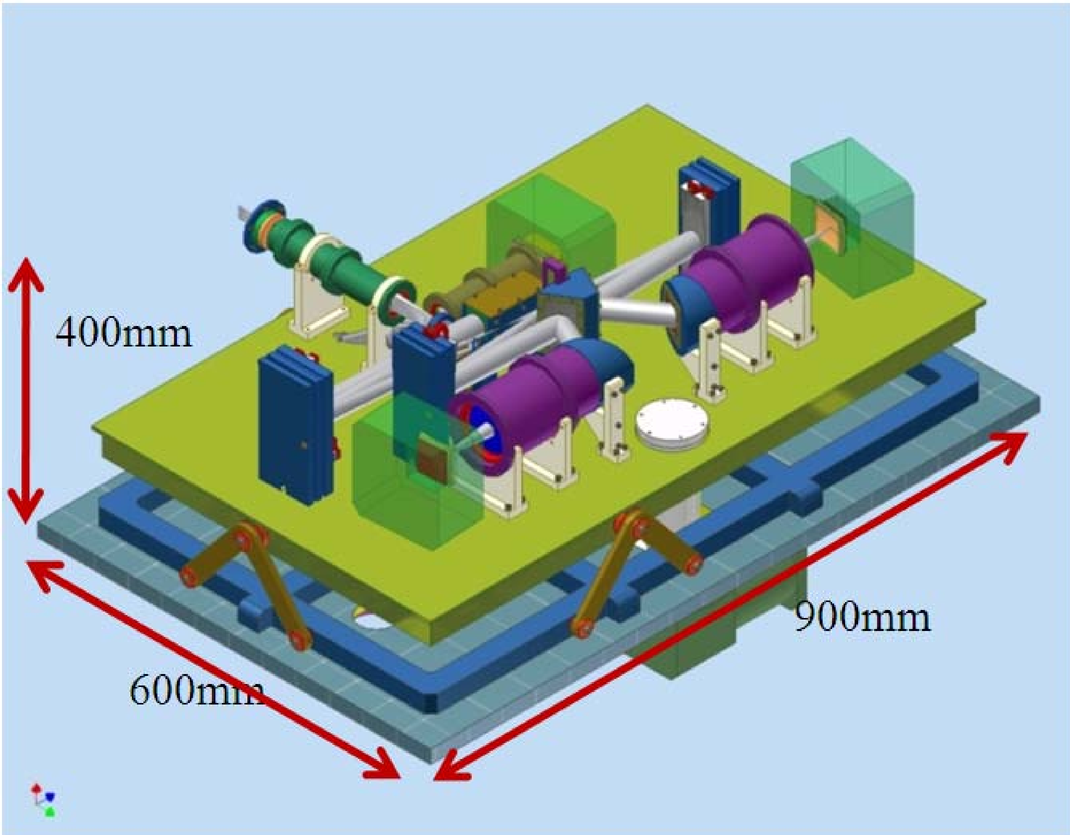

Figure 1. Conceptual design of the cold optics in IGRINS dewar (Jaffe et al. 2009).

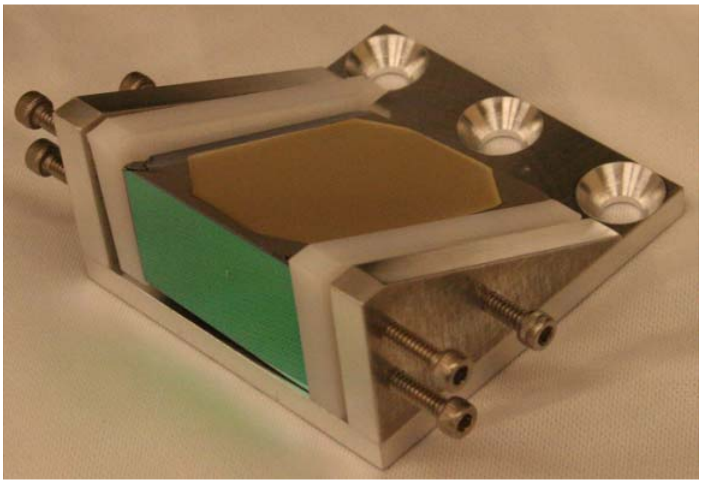

Figure 2. Silicon immersion grating. Incident beam go into the left side surface and the top surface is echelle grating.

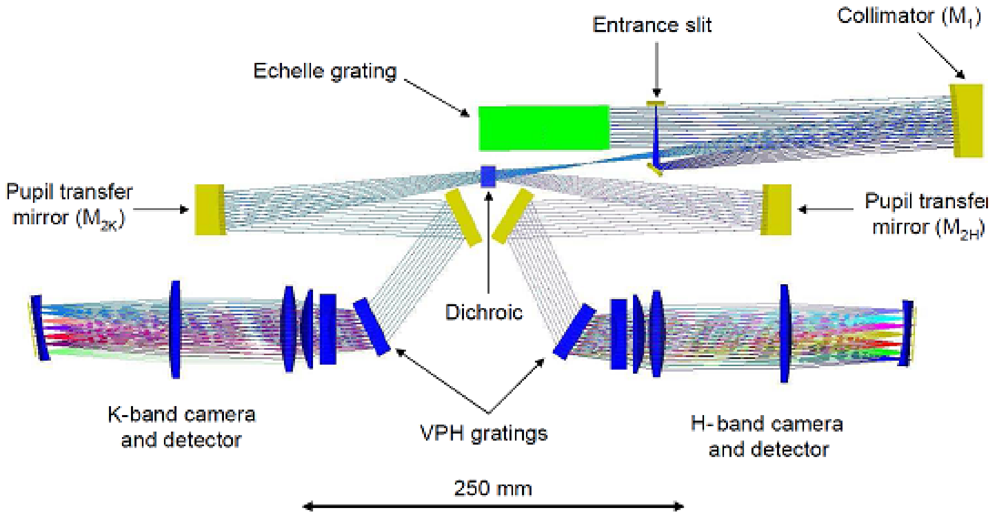

Figure 3. IGRINS optical design (Yuk et al. 2010). *H*-band and *K*-band cameras operate simultaneously to take *H*- and *K*-band spectra in a single exposure.

1.3 Calibration Purpose and Methods

In spectroscopic data reduction, wavelength calibration is essential to correct distortion of spectral image and to determine absolute wavelength of observed source. From the spectrum of various calibration sources, we get *distortion solution* and absolute *wavelength solution*. Adjusting this solution function to object spectra, we can finally get distortion corrected and wavelength identified spectrum.

On the other hand, using the flat frame taken from an artificial blackbody source, we can correct pixel-to-pixel sensitivity variations of detectors and correct intensity non-uniformity which caused by spectroscopic optics. From the flat frame, we can also get *extract solution of echelle order stripes*.

In IR, there are large and variable background emission and absorption than optical ranges (Glass 1999). Therefore, the spectral calibrations in IR are more complicated compare to those of optical wavelength. In general, for the reference line source, artificial illumination lamps are used and also telluric OH emission lines and telluric absorption lines can be used. To provide a blackbody source to the system for flat-fielding, a tungsten halogen lamp with integrating sphere is commonly used. Since IGRINS is very new and innovative high dispersed spectrograph, our calibration system need to achieve high level strategy and should have well based design concept. Among the spectrographs recently developed, we selected several instruments which are cross - dispersed and have high resolving power and we have reviewed their spectroscopic calibration system for the references.

BOES (Bohyunsan Optical Echelle Spectrograph) is a fiber-fed prism cross-dispersed echelle spectrograph installed at the 1.8m telescope of the BOAO (Bohyunsan Optical Astronomy Observatory; Kim et al. 2007). BOES has a resolving power of 30,000 to 90,000 while fiber core size change. BOES obtain a wide wavelength range (0.35 to 1.05 μm) and is using Th-Ar and Th-Ne hollow chathod lamps for the wavelength calibrations.

IRCS (the Infrared Camera and Spectrograph) is facility instrument for the 8.2m Subaru telescope (Tokunaga et al. 1998). IRCS is 1 – 5 μm cross-dispersed echelle spectrograph and has resolving power of 20,000. They use telluric OH emission lines and

Ar lamp for wavelength calibration and tungsten halogen lamp with the gold-coated integrating sphere as a blackbody source.

CRIRES (CRyogenic InfraRed Echelle Spectrograph; Kaufl et al. 2004) is the European Southern Observatory's high resolution (R ~ 100,000) IR spectrograph operating at the Very Large Telescope. Beyond 3 μm, CRIRES can achieve the 85% of calibration process with telluric features and they made an effort on setting the database for the calibration below 3 μm. Kerber et al. 2008 established the infrared spectrum of Th-Ar hollow cathode lamp in the range 900 – 4500 nm for the CRIRES wavelength calibration.

1.5 Purpose of This Work

In this paper, we put efforts to establish the basic calibration concept of IGRINS and the sequence of calibration data process. We select line reference sources which are proper for our high dispersed spectroscopy, and we make a choice for the reference line lamp. For the selection, we compare merits and demerits of cases using each reference source for our instrument. We design a blackbody source for the flat fielding using tungsten halogen lamp and we design the optical system to perform the telescope-simulate calibration beam and to provide uniform flux from the source. Calibration box also be designed containing moving parts to satisfy the hardware requirements according to observation scenario.

2. CALIBRATION CONCEPT FOR IGRINS

2.1 Calibration System Structure

In Figure 4, we showed the conceptual arrangement of the calibration sources. For the IGRINS wavelength calibration sources, we plan to use hallow cathode lamps to get artificial spectral lines emitted by specific elements in the lamp. The telluric OH emission lines which are dominant radiation sources in *J*- and *H*- bands can be also used for the source of wavelength calibrations. In addition, the telluric absorption lines appeared in the spectra of the celestial objects can be another source. In the case of flat-fielding, we will use a tungsten halogen lamp with an integrating sphere to get blackbody radiations and highly uniformed flux at the focal plane. The optics in the calibration system is coupled to the cryogenic relay optics inside the dewar (see Figure 5 for the optical layout).

For observations which require more precise wavelength calibrations, e.g., radial velocity observations, we are considering to adopt a gas absorption cell as an option (Bean et al. 2009). We can use this gas cell as same as the usage of an iodine cell in visible band observations.

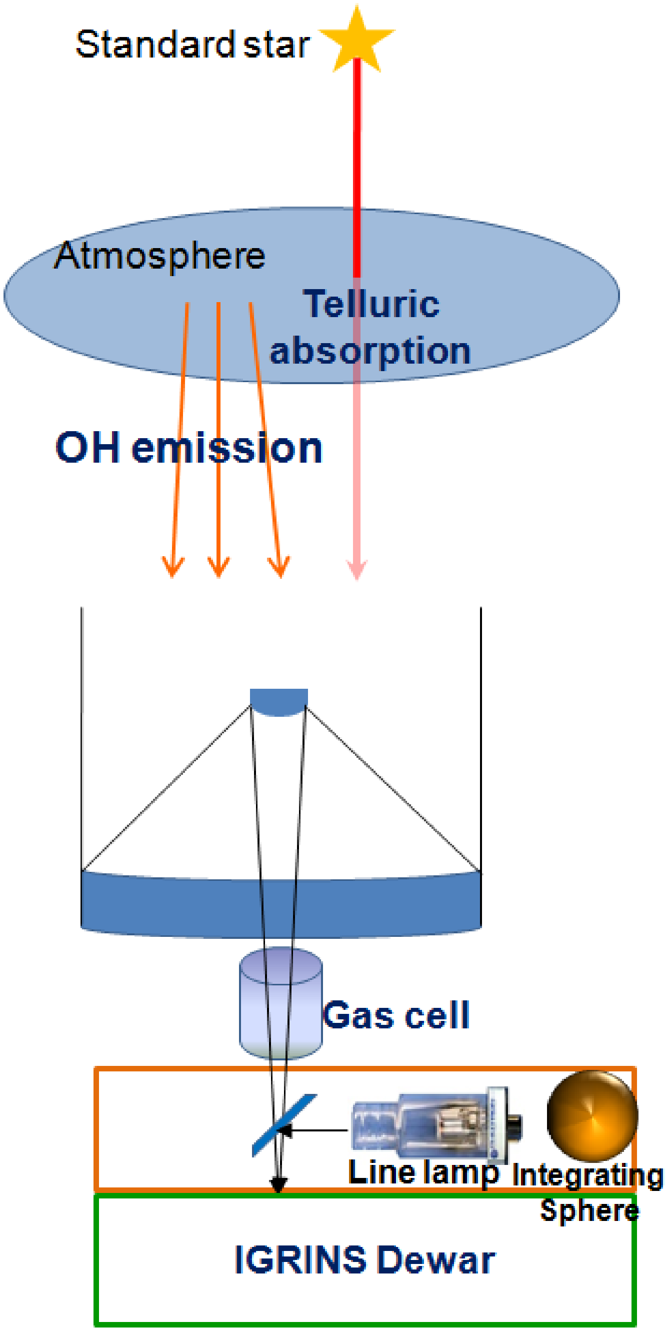

Figure 4. Conceptual arrangement of IGRINS calibration sources.

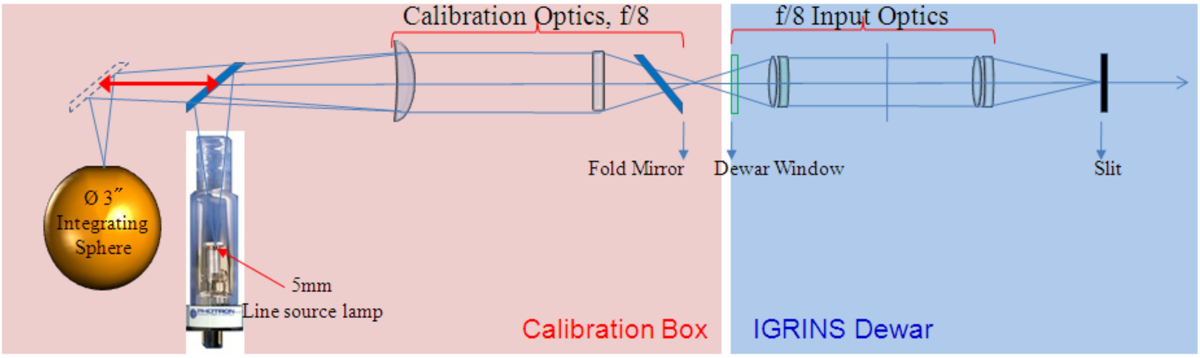

Figure 5. Optical layout of calibration sources. The optical components in the calibration box are in room temperature, and those in the IGRINS dewar are in cryogenic temperature.

2.2 Calibration Sequence

In the Section 2.1, we described the elements in our calibration system. Flat image frames, line lamp frames, and standard star frames taken from observations will be processed by data reduction software (Pak et al. 2009). Figure 6 shows the data reduction sequences (Pyo et al. 2002).

2.2.1 Pre-processing and Flat

All raw image data need to be done by pre-processing routines which correct bad pixels and cosmic-ray events. We also need to correct the pixel-to-pixel responsivity variations and the non-uniformity of the optics. For those corrections, we use a *flat-on* frame and a *flat-off* frame taken by turning on and off the tungsten halogen lamp. The raw flat frames also need to pass the pre-processing routines. By subtracting the flat-off frame from the flat-on frame, we get a *flat* frame and we can have *order extract solution* after flat processes. In addition to the pre-processing routines, all image data will be divided by the *flat* frame.

2.2.2 Line Lamp

By turning on and off the line lamp, we get a *lamp-on* and a *lamp-off* frame. After pre-processing, the lamp-on frame is subtracted by the lamp-off frame and then flat dividing is done. We can extract the order strips of the line lamp frame using the order extract solution from the flat processing. All spectroscopic data have inclination and curvature to the direction of dispersion and also curvature to the slit length direction (Pyo 2002). The relation between the pixel number and distortion can be obtained from the reference source lines. In this step, we also get the absolute wavelength solution. By transforming the non-equal wavelength interval per pixel into equal wavelength interval per pixel and redistribute the pixel value along the wavelength. Now we have *distortion solution* and *wavelength solution*. By converting the 2-dimensional spectra to the 1-dimensional data, we finally get *lamp spectra*.

2.2.3 Standard Star

For telluric transmission correction and for flux calibration, we observe the standard stars, e.g., A0V type stars. Standard star will be taken in the *nod – on – slit mode* of IGRINS (Jaffe et al. 2009). We place the star at one position (*position A*) of slit during the first exposure and we slightly move the telescope along the slit-length direction to place the star at another position (*position B*).

After pre-processing, we subtract *B* from *A* to get the background subtracted standard frame. As we did in the line lamp process, the frame needs to be divided by the flat frame in Section 2.2.1. After flat correction, we extract 1-dimensional echelle order spectra by tracing the stellar continuum emission along the dispersion direction. In this step, we can update *order extract solution*. Then we extract the order aperture strips. Using the distortion solution and the wavelength solution in Section 2.2.2, the strips are transformed to the distortion and wavelength corrected images. We extract 1-dimentialnal stellar spectra of *position A* and *position B* which are combined to get the final standard stellar spectra.

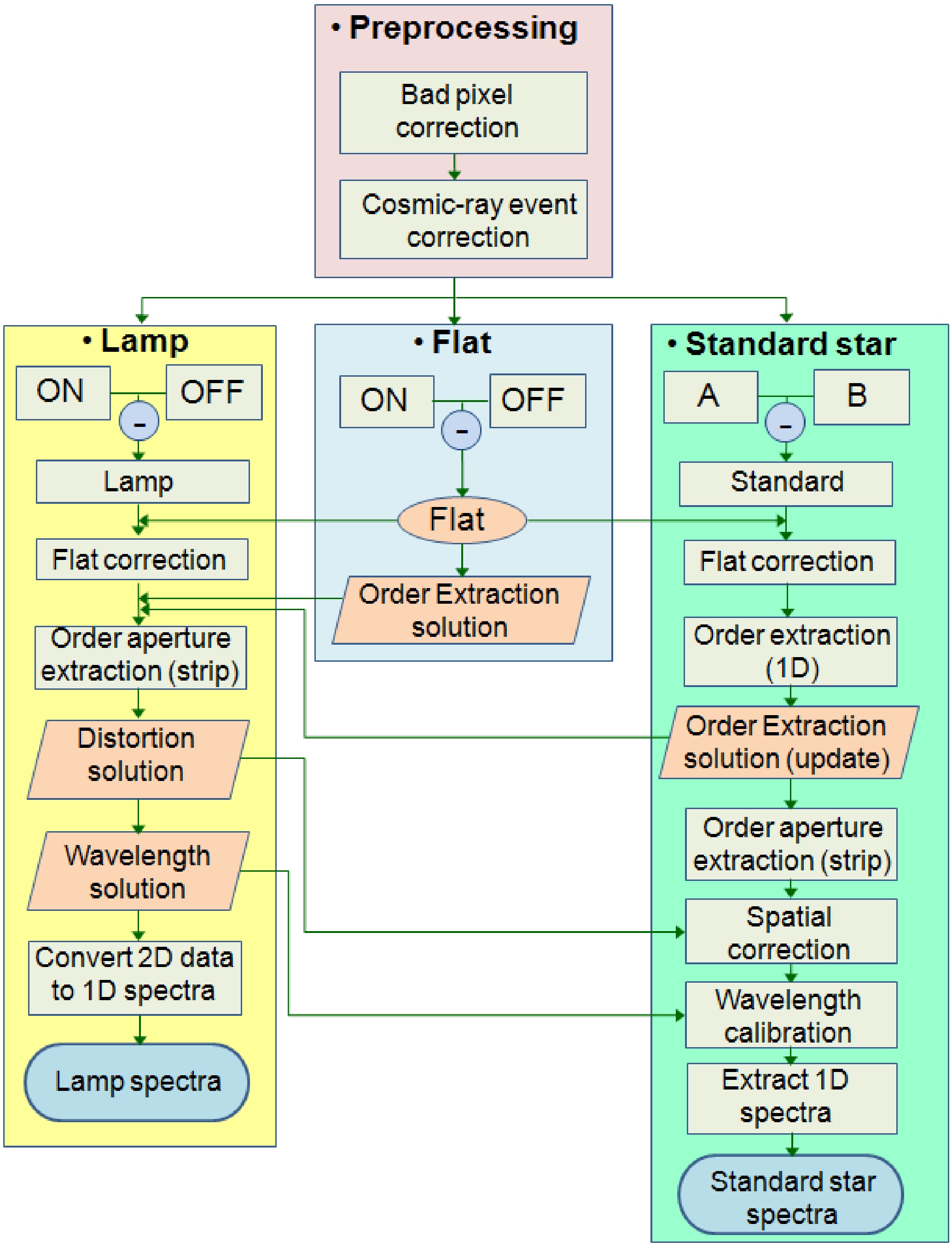

Figure 6. IGRINS data reduction process.

3. WAVELENGTH CALIBRATION

3.1 Echellogram

Echellogram is a diagram that shows how the spectrum orders are spatially distributed in detector array. Spectral images appear with a curvature caused by intrinsic property of spectrograph optics. Figure 7 and 8 shows the echellograms of the *H*- and *K*-band which are plotted using ZEMAX data of spectrograph optics. The rectangles represent the fields of HAWAII 2RG 2048×2048 arrays (or 36.86 × 36.86 mm). IGRINS *H*-band has 23 orders from 1.49μm to1.80μm and *K*-band has 20 orders from 1.96 μm to 2.46 μm. *m* represents a order number of each spectrum, and blaze wavelength λ_B is marked as small circle at echellograms. The order separation Δy_{tot} is denoted in the unit of arcsec. $\Delta\lambda_{FSR}$ is the free spectral range (Figure 7, Figure 8) and two dash dotted lines indicate the free spectral range at each order.

To get the function of distortion and wavelength solution, we need at least three lines per each order to derive quadratic curve solution.

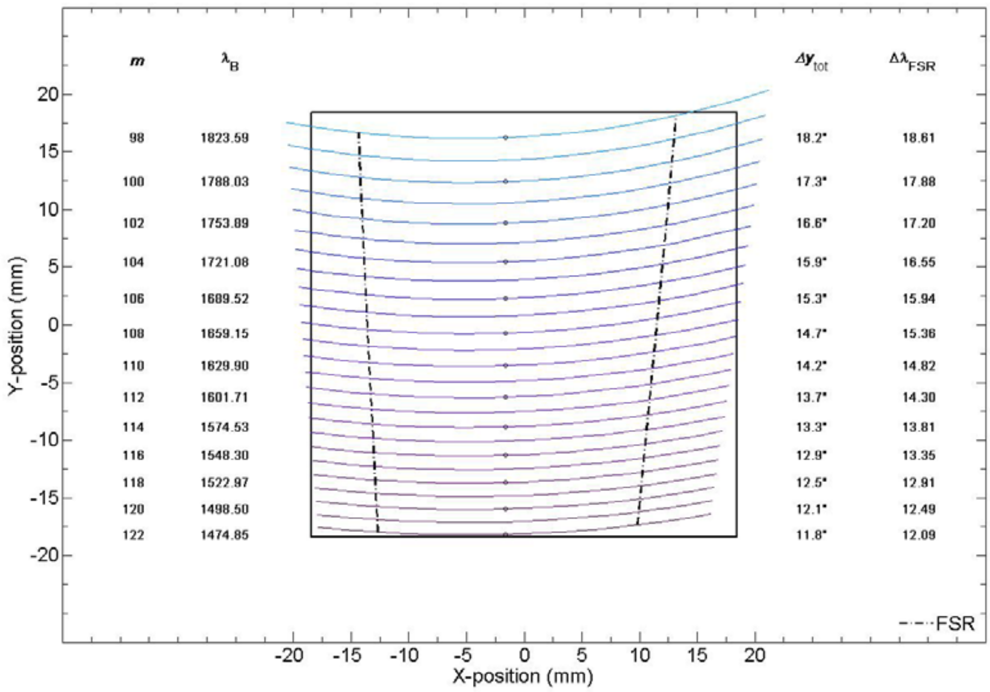

Figure 7. IGRINS H -band echellogram. There are 23 orders from 1.49 μm to1.80 μm. See the detailed explanations in the text (Jaffe et al. 2009).

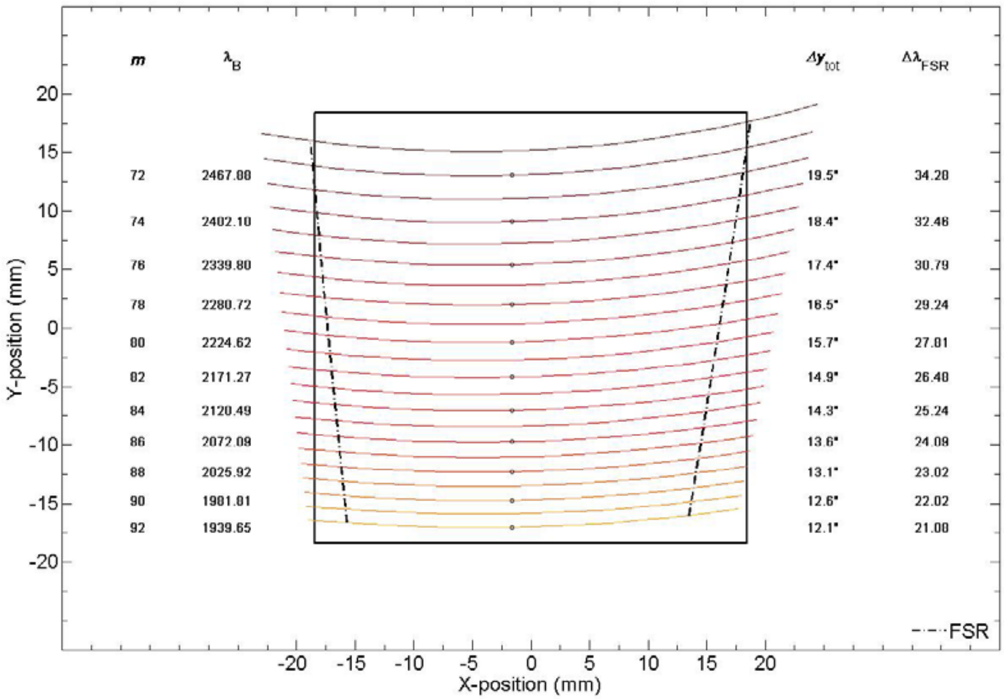

Figure 8. IGRINS *K*- band echellogram. There are 20 orders at 1.96 µm -2.46 µm (Jaffe et al. 2009).

3.2 Sources Selection

In Section 2.1, we listed the various reference sources for the line calibration. Which are

- A hallow cathode lamp – Thorium Argon, Uranium
- OH emission lines
- Telluric absorption lines

Figure 9 shows the distributions of each sources in the range of IGRINS observation wavebands. Th-Ar and uranium cathode lamps shows wide distribution over whole *H*- and *K*- band and the OH emission lines mainly spread in *H*- band. Telluric absorption lines look might be used in several ranges. In this section, we describe the details of each wavelength source and the advantages and disadvantages to determine which will be the best choice for the lien reference source.

3.2.1 Telluric Absorption

The molecules in the Earth's atmosphere (e.g. water vapor, carbon dioxide) make absorption lines in the spectrum of astronomical objects. Figure 10 shows the modeled telluric features in *H*- and *K*- band wavelength. In the process of data reduction, telluric correction function is made by dividing a model spectrum of a star by an observation of astronomical photometric standard stars. The telluric features in standard star spectrum itself can be used as line references for the wavelength calibration. In our application, we will mainly use the telluric absorptions at wavelength longer than 2.2μm, which are caused by water vapor and CO_2. We can use CO_2 lines more usefully because the lines of CO_2 are not changed with place and time, while the lines of H_2O vary with them.

To use the telluric lines, we should set the atmospheric model to predict and to fit those lines with observed spectra. The Standard star observation is essential to use telluric absorption lines as calibration source. Another minor point of adjusting the telluric absorption features to the IGRINS calibration is that telluric lines appear beyond 3 μm much more than below 3 μm. But still we can use several bands of features for particular observing cases.

3.2.2 Telluric OH Emission

In the wavelength range 0.61 - 2.6 μm, there is OH airglow emitted by OH radicals (Rousselot et al, 2000). The emission lines correspond to transitions with Δv= 2 to 5 and it appears as series of band features (Figure 11, 12). The OH radicals are originated in an atmospheric layer of 6 – 10km thickness and its altitude is 85 – 100 km. The airglow emissions should be removed because these lines are typical background noise in IR spectroscopic sky but it can be used as a wavelength calibration source (Oliva & Origlia 1992). We will use the OH line atlas data of Rousselot et al. 2000.

Even though OH emission is very useful since we get emission lines simultaneously by taking object data, still there is disadvantage to select as a main reference for our purpose. OH emissions are dominant mainly in *H*- band and number of lines are decrease at *K*- band (Glass 1999) so we cannot use only OH emission lines at whole *H*- and *K*- band area.

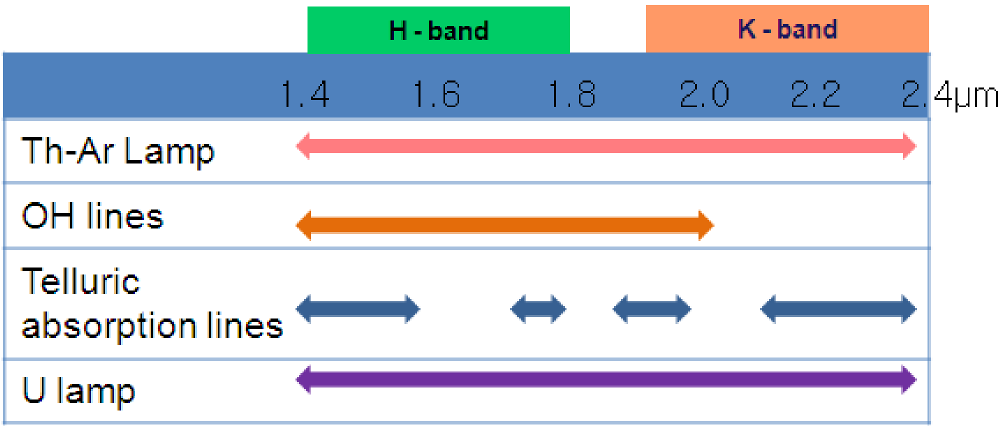

Figure 9. Source line allocation in IGRINS wave bands.

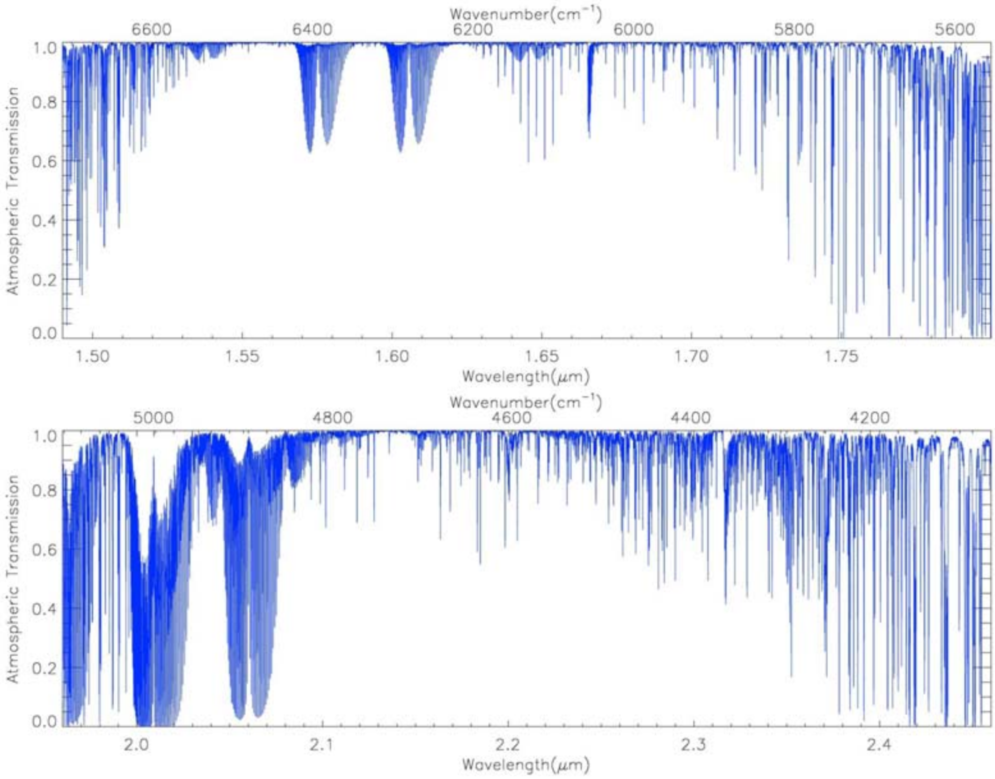

Figure 10. Telluric features at *H*- and *K*- band. (Seo et al. 2010)

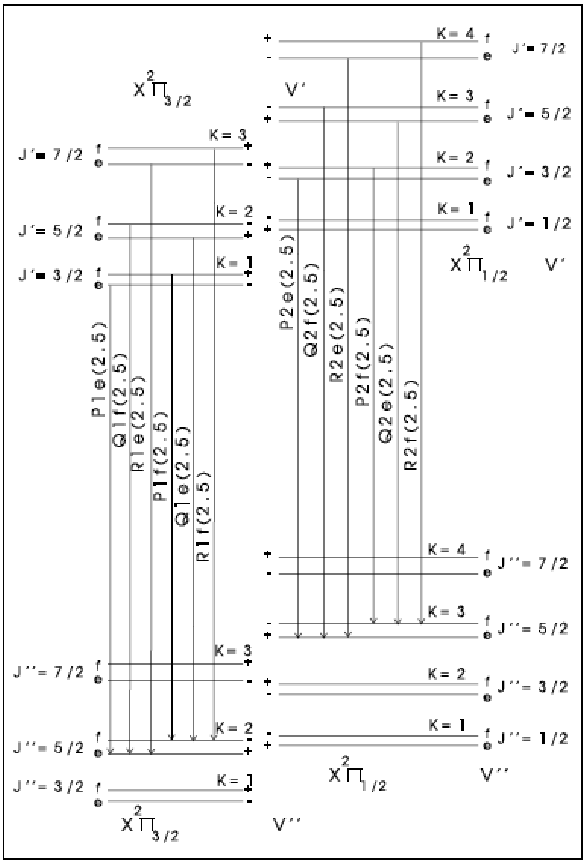

Figure 11. Various OH molecule transition processes caused by rotation – vibration band (Rousselot et al. 2000) in infrared.

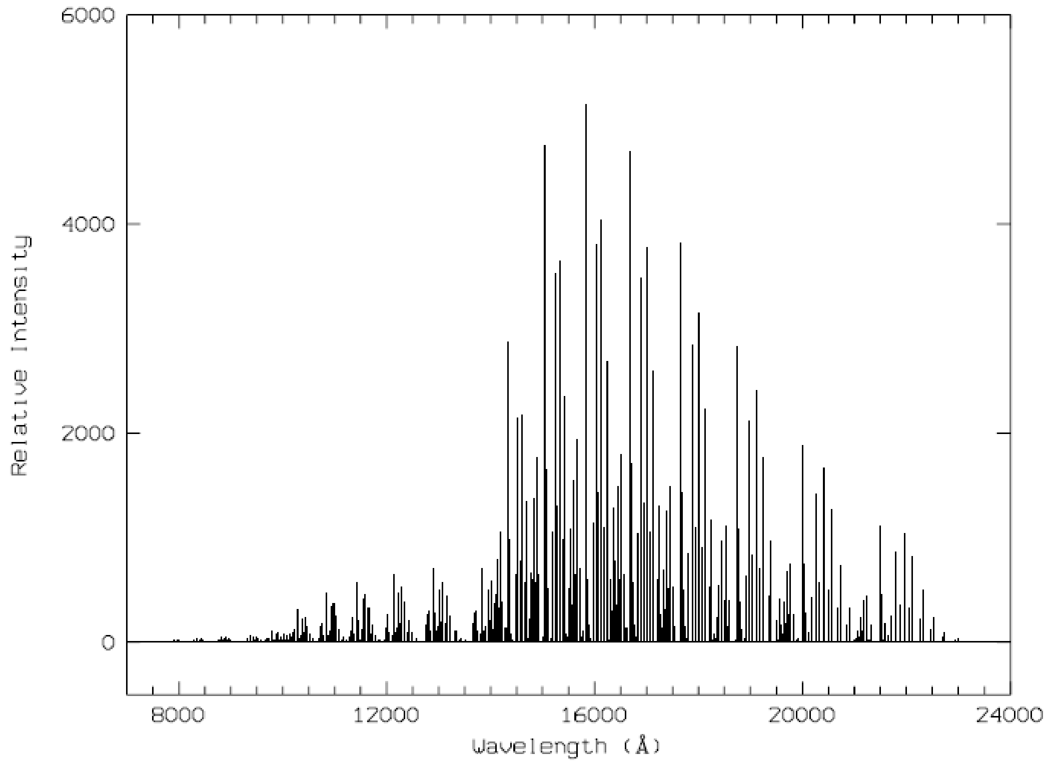

Figure 12. OH band features appeared in *H*- and *K*- band wavelength (Rousselot et al. 2000).

3.2.3 Th-Ar Lamp

Th-Ar hollow cathode lamp is well known as a calibration reference source at visible and near infrared bands. The lamp has thorium filament and is filled with argon gas. Kerber et al. 2008 has established more than 2400 lines that are suitable for wavelength standards in the range of 900-4500 nm and the line list is used for the wavelength calibration of CRIRES (Cryogenic High-Resolution IR Echelle Spectrometer). BOES (Bohyunsan Optical Echell Spectrograph) also uses Th-Ar lamp as a calibration source at optical band. We used the established line data of Kerber et al. (2008) for our *H*- and *K*-band application. But there is lack of emission lines from Th-Ar lamp beyond 2.2 μm range.

Th-Ar lamp is convenience because it has been commonly used and there already enough establish data is exists. We can take the lamp frame not only in observing time but during daytime and we can measure its spectrum even by laboratory experiment. In the other hand, we need to construct particular calibration structure to make a use of this artificial line emitting source.

3.2.4 Uranium Lamp

Uranium has a denser emission lines in spectrum than thorium and has been used as a calibration standard (Engleman et al, 2002). Palmer et al. 1980 published the near-ultraviolet and visible spectrum of uranium-neon hollow cathode lamp and Conway et al. 1984 classified 4418 uranium spectrum and 4744 unclassified spectrum between 1.8 and 5.5 microns emitted from a hollow cathode.

In astronomical wavelength calibration, uranium lamp has not been used as a prefer source while Th-Ar is widely used. But there is an example that is the wavelength calibrations of SOLIS ISS (Integrated Sunlight Spectrometer) at NSO is being done by U-Ar lamp (Keller 2000) in the wavelength range 0.35 to 1.1 μm. Since the high resolution infrared instruments as recently developed, now we need to find more proper source to provide more accurate calibration process in the infrared range. Thus, we tried to confirm whether the uranium lamp can be used for line calibration or not by counting the number of available lines at each IGRINS order (Figure 15, Figure 16). We used the line data of Conway et al. 1984 in *K*- band and we do not have the uranium spectrum in *H*- band yet.

3.2.5 Number of Lines and Choice of Lamp

H- and *K*- bands spectra of IGRINS have 23 and 20 orders respectively and we need to have more than 3 lines in each order. Using Th-Ar, OH, and U line data (Section 3.2.2, 3.2.3, 3.2.4), we plotted histogram to show the number of source lines considering dynamic intensity range within $10^{2.5}$. Figure 13 – 15 shows the number of lines and marked squares represent the intensity range we selected. In Table 2 – 6 we listed line list which are in the selected intensity range in Figure 13 – 15. In table 2 – 5, intensities are displayed as log scales and the absolute flux is arbitrary. In table 6, intensities are shown by integers and increment of 1 represents a factor of 3 increases in intensities. Spectral values partitioned by dotted lines represent the lines located in the overlapped ranges of previous and following orders. We also counted the number of lines at each order to check whether we have enough lines or not for each source (Figure 16). Even though Th-Ar and OH lines cover the whole *H*-band and the most of *K*- band orders, there are not enough reference lines at the ends of *K*- band. In the range of 2.3 – 2.5 μm of the *K*- band where has the longest wavelength in our instrument, the Th-Ar and OH lines significantly decrease while the U lamp still has 8 -14 lines at each order.

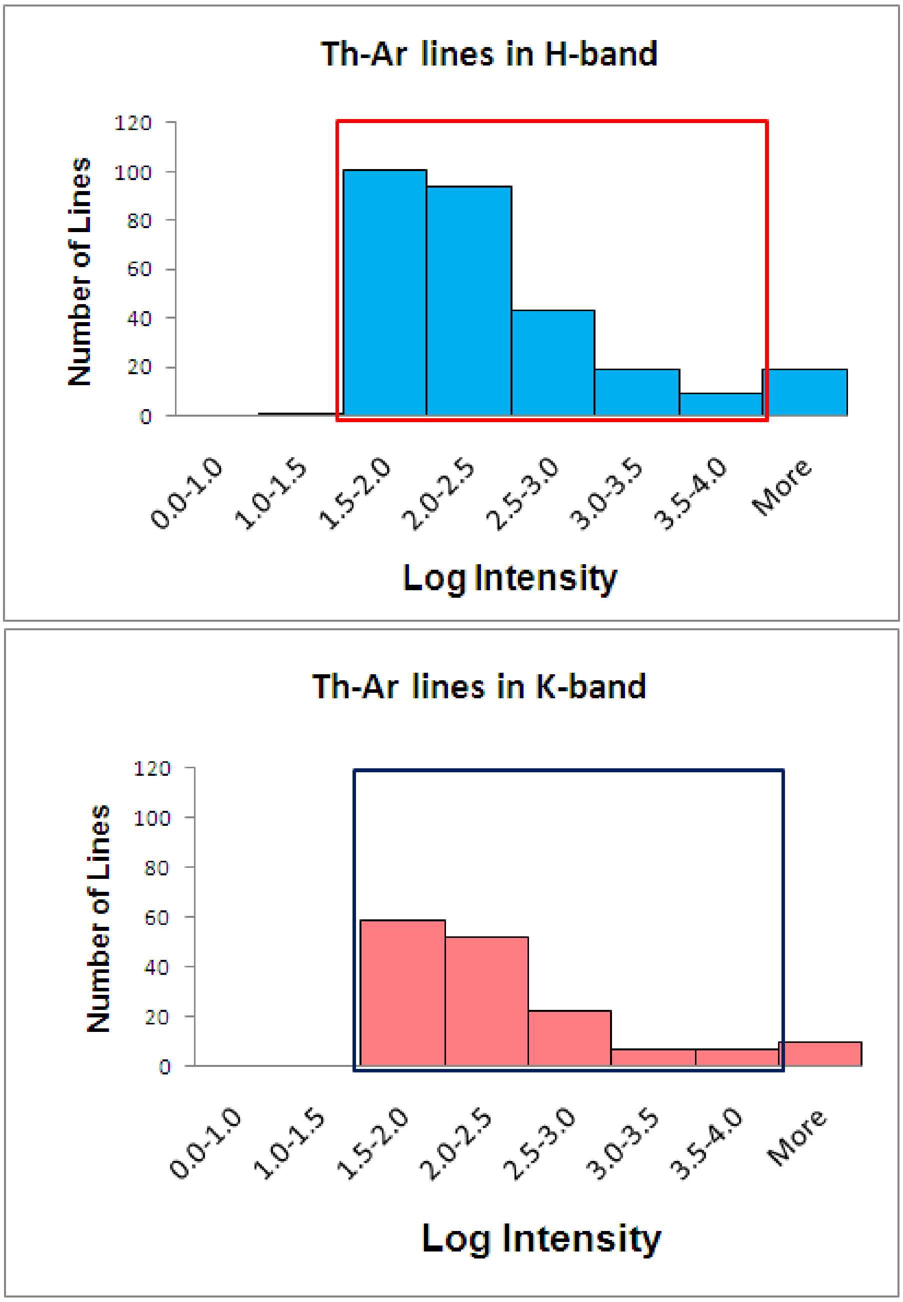

Figure 13. Number of Th-Ar lines in *H*- and *K*- band. Considering dynamic range of the detector, we select lines within $10^{2.5}$ ranges.

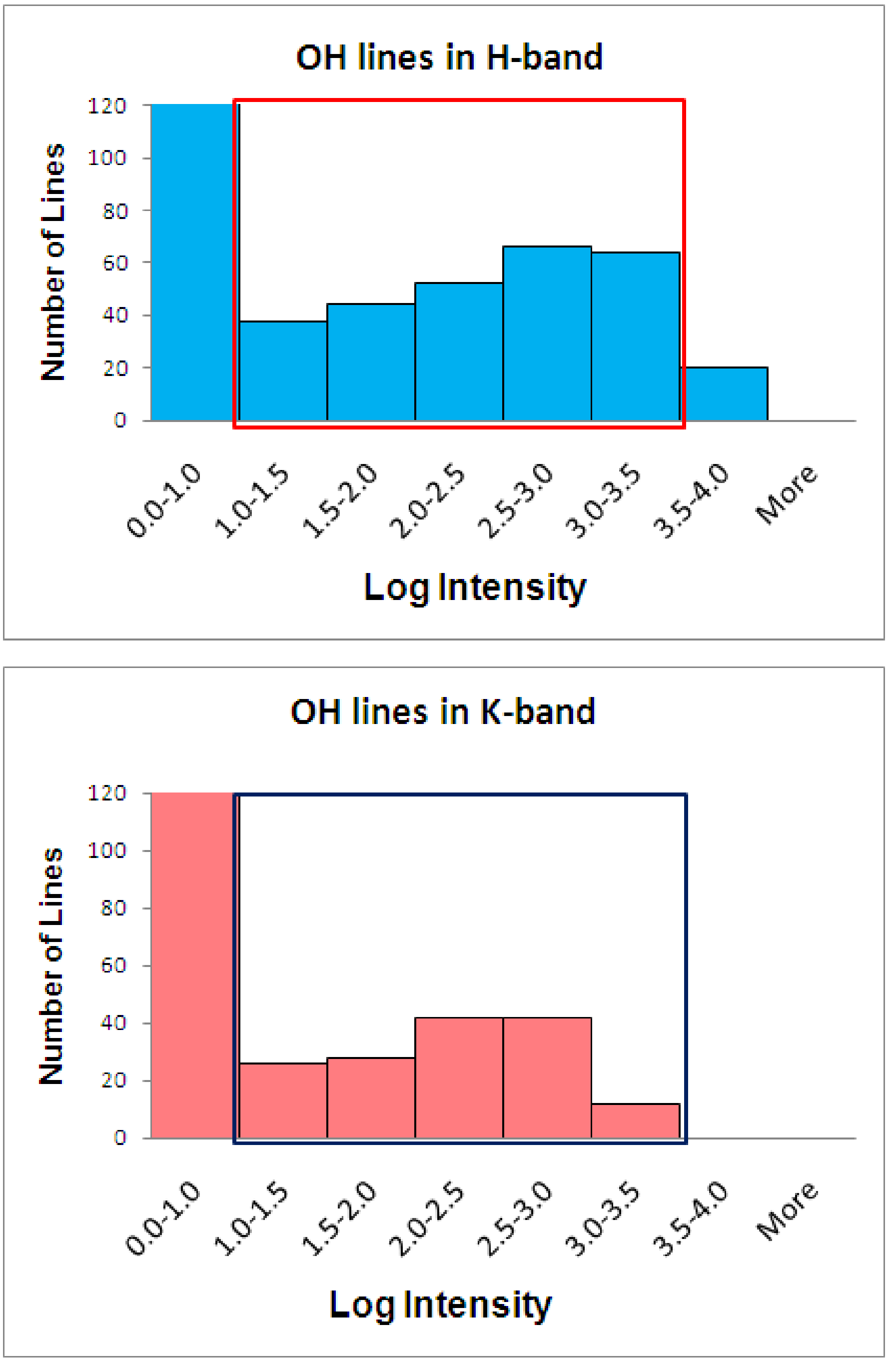

Figure 14. Number of OH emission lines in *H*- and *K*- band.

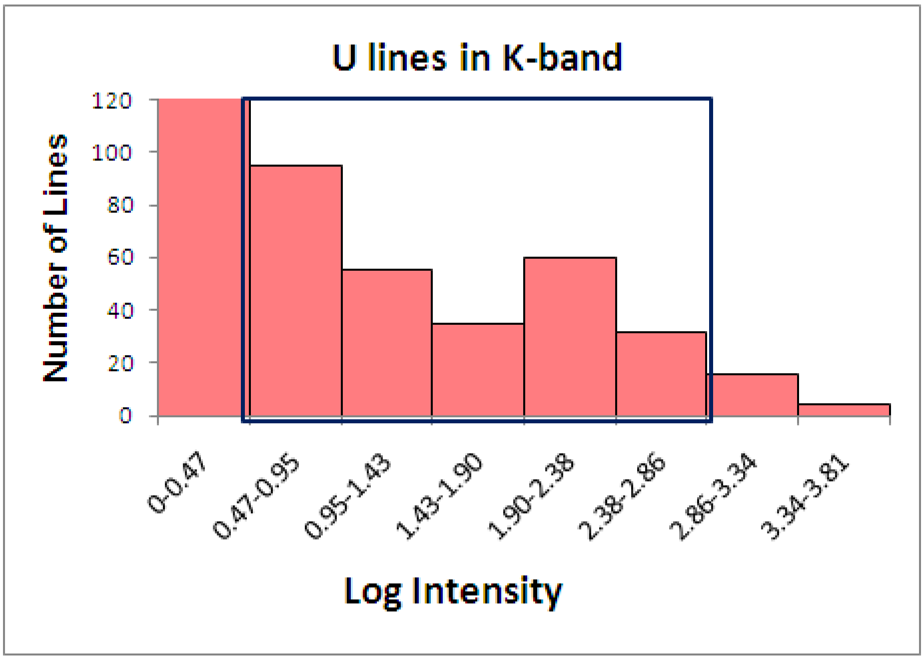

Figure 15. Number of uranium lines in *K*- band. We selected lines within 3^5 ranges.

Table 2

Th-Ar lines in *H*- band (Kerber et al. 2008)

Order No.	lambda (nm)	Species	Intensity[a]
122 (1468.81-1480.90)	1468.1258	ThI	3.0
	1469.9592	ThI	2.3
	1470.6779		1.6
	1471.8662		1.7
	1472.0378	ThI	2.0
	1472.2814	ThI	3.0
	1472.3463	ThI	1.9
	1474.3167	ArI	4.0
	1474.5356	ThI	2.9
	1476.0655	ThI	2.3
	1476.8777	ThI	2.0
	1477.6056	ThI	2.1
	1478.1263	ThI	1.6
	1480.1922	ThI	2.1
121 (1480.44-1492.72)	1480.9465	ThI	2.3
	1481.0507	ThI	3.1
	1481.3079	ThI	1.7
	1483.4049	ThI	1.7
	1483.4268	ThI	2.1
	1491.4511	ThI	1.9
	1491.5069	ThI	1.7
	1491.5120	ThI	1.9
120 (1492.26-1504.75)	1493.2569	ThI	2.4
	1493.3118	ThI	2.5
	1494.4584	ThII	2.6
	1494.8068	ThI	3.3
	1495.1388	ThI	2.1
	1497.2578	ThI	1.7
	1497.4848	ThI	1.7
	1497.8662	ArI	2.4
	1498.0935		1.6
	1498.1416	ThI	2.4
	1498.8984	ThI	2.6
	1499.2696	ThII	2.4
	1499.8652	ThI	1.9
	1499.8755	ThI	2.2
	1501.4127	ThI	2.1
	1502.5904	ThI	2.1
	1503.4622	ArI	3.6
119 (1504.29-1516.98)	1504.9518	ThI	2.3
	1505.3777	ThI	1.9
	1505.6058	ThII	1.9
	1505.6679	ArI	2.4

Table 2

(Continued)

Order No.	lambda (nm)	Species	Intnesity[a]
119 (1504.29-1516.98)	1506.9835	ThI	1.9
	1509.4934	ThI	1.9
	1509.9489	ThI	1.7
	1510.0136		2.0
	1510.3453	ThI	2.5
	1510.4952	ThI	1.9
	1511.6611	ThI	2.1
	1514.7483	ThI	1.9
118 (1516.52-1529.42)	1519.3006	ThII	2.5
	1519.4503	ThI	1.6
	1519.4925	ThI	2.2
	1523.4196		1.9
	1524.3451	ThI	2.4
	1524.4417	ThII	2.4
	1526.8520	ThI	1.8
	1527.7500	ThI	2.1
	1528.6209	ThI	1.7
117 (1528.96-1542.09)	1529.5387	ThI	1.9
	1529.6678	ThI	2.0
	1531.1472	ThI	3.2
	1532.0121	ThII	2.0
	1533.3535	ArI	4.3
	1535.7322	ArI	4.0
	1535.9883	ThI	2.9
	1539.9919	ThI	2.0
116 (1541.62-1554.97)	1543.3996	ThI	3.7
	1544.3765	ThI	1.9
	1544.4328	ThI	2.7
	1547.7090	ThI	2.2
	1547.7540	ThI	1.8
	1552.0673	ThI	3.0
	1552.7393	ThI	1.7
115 (1554.51-1568.09)	1554.6908	ThI	1.9
	1555.5924	ThI	2.3
	1555.7490	ThI	1.8
	1555.9712	ArI	3.0
	1556.3809		2.1
	1557.3752	ThI	2.2
	1557.6369	ThI	2.6
	1557.6614	ThI	1.8
	1558.0120	ThI	1.7
	1558.0831	ThI	3.2
	1558.7889	ThI	1.9

Table 2
(Continued)

Order No.	lambda (nm)	Species	Intensity[a]
115 (1554.51-1568.09)	1558.9479	ThI	2.1
	1560.2936	ThI	2.5
	1560.3084	ThI	2.3
	1561.2410	ThI	1.7
	1561.3194	ThI	1.9
	1563.2541	ThI	2.0
	1563.8748	ThI	2.1
	1564.4720	ThII	2.2
	1564.5604	ThI	2.1
114 (1567.62-1581.43)	1568.0439	ThI	2.1
	1570.5589	ThI	2.2
	1571.7440	ThI	2.5
	1573.9207	ArI	3.2
	1574.8181	ThI	2.0
	1577.1870	ThII	1.6
	1578.0922	ArI	2.6
113 (1580.97-1595.03)	1581.9815	ThII	2.3
	1582.9498	ThI	2.0
	1583.6071	ThI	3.5
	1585.2053	ThI	2.0
	1588.7506	ArI	3.6
	1589.5904	ThI	2.3
	1589.6193	ThI	2.2
	1590.3883	ThI	2.3
	1592.6474	ThI	2.3
	1593.6770	ThII	2.2
	1594.0420	ThI	2.0
112 (1594.56-1608.86)	1595.8805	ThI	2.4
	1596.4376	ThI	2.1
	1598.2757	ThI	2.0
	1600.2204	ThI	1.9
	1601.0126	ThI	2.7
	1601.2688	ThI	1.9
	1601.8791	ThI	1.8
	1603.7535	ThI	1.7
	1604.2885	ThI	2.2
	1607.6370	ThI	1.7
	1607.6978	ThI	2.0
111 (1608.40-1622.96)	1611.4191	ThI	2.9
	1612.7063	ArI	3.7
	1614.7168	ThI	1.9
	1615.2000	ThI	2.2
	1618.2880	ThI	1.9
	1618.4441	ArI	4.0
110 (1622.49-1637.31)	1622.5159	ThI	2.4
	1624.2562	ThI	2.1
	1624.4895	ThII	2.0
	1626.8511	ArI	3.3

Table 2
(Continued)

Order No.	lambda (nm)	Species	Intensity[a]
110 (1622.49-1637.31)	1628.4727	ThI	2.2
	1630.8588	ThI	2.2
	1631.3039	ThI	1.6
	1631.5151	ThI	2.1
	1633.4268	ThI	1.7
	1634.5209	ThI	2.0
	1636.8092	ThI	1.6
109 (1636.85-1651.93)	1638.5386	ThII	2.4
	1641.7292	ThI	2.3
	1650.8303	ThI	2.4
108 (1651.47-1666.83)	1653.8840	ThI	2.0
	1654.2908	ThI	1.9
	1654.4937	ThI	2.8
	1659.2353	ThI	2.2
	1659.4086	ThI	1.6
	1659.6644	ThI	2.0
	1660.3889	ThI	2.1
	1662.9152	ThI	1.7
107 (1666.37-1682.02)	1670.9206	ThI	2.2
	1671.7000	ThI	2.1
	1673.4585	ThI	1.9
	1675.2072	ThI	1.8
	1675.3019	ThI	2.6
	1677.3128	ThI	3.1
	1678.9642	ThI	2.0
	1678.9799	ThI	1.8
106 (1681.55-1697.49)	1682.5524	ThI	2.4
	1685.7228	ThI	1.9
	1686.4699	ArI	2.6
	1688.3908	ThII	1.9
	1689.4681	ThII	2.0
	1694.3354	ThI	2.2
105 (1697.03-1713.27)	1698.1728		2.0
	1700.9339	ThI	2.1
	1701.3193	ThI	1.8
	1708.0405	ThI	2.0
	1708.3456	ThI	2.3
	1708.3719		1.9
	1709.2997	ThI	1.8
	1711.8210	ThI	1.9
	1712.5984	ThI	2.0
104 (1712.80-1729.35)	1713.8835	ThI	2.4
	1714.0008	ThI	2.5
	1714.7763		1.9
	1714.9894	ThI	1.9
	1717.0449	ThI	1.8
	1719.1581	ThI	1.9
	1721.2176		1.7

Table 2
(Continued)

Order No.	lambda (nm)	Species	Intensity[a]
104 (1712.80-1729.35)	1721.2922	ThII	2.5
	1723.0365	ThI	1.9
	1726.8875	ThI	2.2
	1727.2644	ThI	2.2
103 (1728.89-1745.76)	1731.2385	ThI	3.5
	1738.5348	ThI	2.8
	1738.6653	ThI	3.6
	1739.0107	ThI	2.6
	1739.9322	ThI	1.8
	1740.9075	ThI	2.5
	1745.0012	ThI	3.4
102 (1745.29-1762.49)	1747.8469	ThI	1.7
	1748.5826	ThII	3.3
	1751.3129	ThI	1.7
	1752.6507	ThI	1.6
	1753.9303	ThII	2.0
	1755.7456	ThI	2.2
	1757.7910	ThI	2.2
	1758.9310	ThI	3.5
101 (1762.03-1779.56)	1762.7900	ThI	3.2
	1763.0844	ThI	2.0
	1763.7357	ArII	1.9
	1763.9141	ThI	2.1
	1765.4292	ThI	1.7
	1767.4425	ThI	1.8
	1768.2302	ThI	1.9
	1768.8645	ThI	2.0
	1769.3572	ThI	1.8
	1770.1255	ThI	2.0
	1770.8501	ThI	2.2
	1772.5187	ThI	2.0
	1774.9743	ThI	2.8
	1776.1940	ThI	1.6
	1778.8018	ThI	2.6
100 (1779.09-1796.97)	1779.3058	ThI	1.8
	1783.0740	ThI	2.7
	1786.1375	ArII	1.8
	1787.8471	ThI	1.8
	1788.7925	ThI	1.6
	1789.1555	ThI	2.0
	1789.2850	ThI	2.0
	1791.0201	ArII	2.2
	1794.1337	ThII	2.3
	1795.0665		2.0
	1796.0764	ThI	1.8
99 (1796.51-1814.75)	1796.9822	ThI	2.8
	1798.1879	ThI	2.2
	1799.8698	ThI	2.1

Table 2
(Continued)

Order No.	lambda (nm)	Species	Intensity[a]
99 (1796.51-1814.75)	1801.2480	ThI	2.0
	1802.9995		1.9
	1803.4550		1.9
	1807.7266	ThI	2.7
	1810.8044	ThI	2.1
	1813.0910	ThI	2.8
98 (1814.28-1832.89)	1816.6530	ThI	1.8
	1824.4400	ThII	2.0
	1827.6368	ThII	1.9
	1828.9639	ThI	1.9

[a] The intensity values are in arbitrary units in log scales.

Table 3

Th-Ar lines in *K*- band (Kerber et al. 2008)

Order No.	lambda (nm)	Species	Intensity[a]
92 (1928.11-1950.19)	1931.4457	CaI	2.9
	1932.3149	ThI	1.9
	1934.4264	ThII	2.4
	1939.6613	ThI	2.1
	1940.2069	ThI	1.9
	1940.5762	ThI	2.2
	1943.3109		1.9
	1945.8289	CaI	3.2
	1948.2073	ThI	2.0
91 (1949.73-1971.27)	1951.1053	CaI	2.7
	1960.0416	ThI	2.3
	1962.2494	ThI	1.9
	1964.4249	ArII	2.2
	1964.9890	ThII	1.7
	1967.3821	ThI	2.7
	1967.5264	ThI	1.9
	1967.9885	ThI	2.1
	1968.8596	ThII	2.5
	1968.8796	ThII	1.8
90 (1970.80-1992.82)	1974.6811	ThI	2.7
	1977.0562	ThI	2.1
	1977.9702	ThII	2.2
	1978.2176	CaI	3.5
	1979.1423	ThI	2.5
	1985.8316	ThI	1.8
	1986.3080	ThI	1.8
	1986.7608	CaI	2.7
	1988.7714	ThI	1.8
	1990.8136	ThI	2.2
	1990.8552	ArI	2.6
89 (1992.36-2014.87)	2001.0898	ThII	2.6
	2003.1572	ThI	1.9
	2005.3415	ThI	1.9
	2008.2868	ThI	2.0
	2013.4197	ThI	2.1
88 (2014.41-2037.43)	2019.6887	ThI	2.2
	2030.6453	ThII	1.7
	2032.2554	ArI	3.9
	2032.3300	ThI	2.3
87 (2036.96-2060.51)	2038.3448	ThI	1.6
	2038.6862	ThI	2.1
	2042.7321	ThI	1.8
86 (2060.05-2084.14)	2064.0010	ThI	3.0

Table 3

(Continued)

Order No.	lambda (nm)	Species	Intensity[a]
86 (2060.05-2084.14)	2068.5762	ThI	2.6
	2069.7724	ThII	2.1
85 (2083.68-2108.34)	2086.8262	ThI	1.7
	2087.5145	ThI	2.8
	2088.5269	ThI	1.8
	2095.7188	ThI	1.7
	2099.2703	ThII	1.9
	2102.5256	ThI	2.0
	2105.5955	ThI	2.2
84 (2107.87-2133.11)	2110.1546	ThII	2.0
	2113.8418	ThI	1.8
	2114.8958	ThI	2.3
	2115.4262	ThI	2.1
	2116.8468	ThII	2.1
83 (2132.65-2158.50)	2133.8709	ArI	3.6
	2135.9027	ThI	2.1
	2138.0941	ThI	2.1
	2141.2592	ThI	1.6
	2142.4553	ThI	1.7
	2147.8709	ThI	1.7
82 (2158.03-2184.51)	2161.1532	ThI	1.8
	2163.4918	ThI	2.5
	2164.3164		2.1
	2166.1268	ThI	1.5
	2166.1659	ThI	1.9
	2167.5908	ArI	2.0
	2171.8512	ThI	2.5
	2174.9931	ThII	2.9
	2175.3264	ThI	1.9
	2177.0260	ArII	2.5
81 (2184.05-2211.18)	2194.7810	ArII	2.4
	2195.0934	ThI	2.3
	2196.5373	ThI	1.7
	2197.9070		1.7
	2199.6726	ThI	1.9
	2204.5577	ArI	3.7
	2207.9530	ThI	1.6
80 (2210.71-2238.52)	2210.9662	ThI	2.6
	2227.0412	ThII	2.1
	2235.0862	ThI	2.0
79 (2238.05-2266.56)	2238.3878	ThI	1.7
	2250.2938	ThI	2.1
	2254.3916	ThI	2.3

Table 3

(Continued)

Order No.	lambda (nm)	Species	Intensity[a]
79 (2238.05-2266.56)	2262.0549	ThI	2.5
	2265.2368	ThI	2.2
78 (2266.10-2295.34)	2271.6377	ThI	2.1
	2283.5741	ThI	1.8
	2284.0812	ThI	1.8
	2285.0178	ThI	1.7
	2285.7858	ThI	1.9
	2286.1403	ThI	1.9
	2287.0343	ThI	2.3
	2290.7145	ThI	1.9
77 (2294.87-2324.87)	2297.1016	ThI	1.7
	2315.9926	ThI	2.7
	2318.1779	ThI	2.1
	2322.5144	ArII	2.2
76 (2324.40-2355.19)	2327.6449	ThI	1.7
	2333.7035	ThI	1.9
	2337.2390	ArII	2.1
	2344.3913	ThII	2.1
	2352.1172	ThI	2.7
75 (2354.72-2386.33)	2355.8046	ThI	1.6
	2366.9928	ThI	1.8
	2367.9292	ThI	1.8
	2371.1241	ThI	1.6
	2378.8325	ThI	2.6
74 (2385.86-2418.33)	2391.3668	ThI	1.7
	2401.4515	ThI	2.3
	2414.2839	ThI	2.1
73 (2417.86-2451.21)	2417.9461	ThI	2.0
	2430.8477	ThI	1.7
	2443.5247	ThI	1.8
	2447.5408	ThII	2.1
72 (2450.74-2485.02)	2479.6111	ThI	1.9
	2481.3761	ArII	2.1
71 (2484.55-2519.79)	2490.9163	ThI	1.7
	2493.8129	ThI	1.8
	2500.4325	ThI	1.8
	2505.6432	ThI	1.9
	2508.7502	ThI	2.0

[a] The intensity values are in arbitrary units in log scales.

Table 4

OH lines in *H*- band (Rousselot et al. 2000)

Order No.	lambda (nm)	Intensity[a]
122 (1468.81-1480.90)	1467.0310	1.1
	1467.0979	1.1
	1469.7998	3.1
	1469.8876	3.1
	1470.1920	1.8
	1470.2563	1.8
	1471.3085	1.5
	1471.3528	1.5
	1473.9721	2.4
	1474.0309	2.4
	1475.5427	2.1
	1475.5751	2.1
	1477.2176	2.5
	1477.2590	2.5
	1478.3486	2.8
	1478.3987	2.8
	1479.9240	2.8
	1480.0423	2.8
121 (1480.44-1492.72)	1480.5702	2.5
	1480.5877	2.5
	1483.2902	3.1
	1483.3285	3.1
	1486.4397	2.8
	1486.4397	2.8
	1488.5823	2.0
	1488.6508	2.0
	1488.7579	3.2
	1488.7819	3.2
	1490.8278	2.3
	1490.9776	2.3
120 (1492.26-1504.75)	1493.1795	2.8
	1493.1971	2.8
	1500.6255	1.4
	1500.7219	1.4
	1502.5143	1.7
	1502.6969	1.7
119 (1504.29-1516.98)	1505.2850	2.7
	1505.2882	2.7
	1506.3975	2.2
	1506.4021	2.2
	1506.8938	3.2
	1506.8998	3.2
	1508.2237	1.8

Table 4

(Continued)

Order No.	lambda (nm)	Intensity[a]
119 (1504.29-1516.98)	1508.2272	1.8
	1508.8211	2.7
	1508.8341	2.7
	1510.7382	1.3
	1510.7382	1.3
	1511.3615	2.1
	1511.3835	2.1
	1514.5333	1.5
	1514.5663	1.5
118 (1516.52-1529.42)	1518.7009	3.0
	1518.7271	3.0
	1524.0788	3.5
	1524.1120	3.5
	1528.7747	3.1
	1528.7831	3.1
117 (1528.96-1542.09)	1539.5258	3.0
	1539.5411	3.0
116 (1541.62-1554.97)	1542.9836	1.2
	1543.0490	1.2
	1543.1701	3.4
	1543.2612	3.4
	1546.1807	1.9
	1546.2443	1.9
	1547.3985	1.6
	1547.4439	1.6
	1550.0571	2.4
	1550.1157	2.4
	1550.9559	2.7
	1550.9979	2.7
	1551.7706	2.2
	1551.8039	2.2
	1553.9711	3.0
	1554.0945	3.0
115 (1554.51-1568.09)	1554.5890	2.9
	1554.6393	2.9
	1557.0070	2.6
	1557.0249	2.6
	1559.7439	3.2
	1559.7823	3.2
	1563.0972	2.3
	1563.1560	2.8
	1563.1563	2.8
	1563.1677	2.3

Table 4
(Continued)

Order No.	lambda (nm)	Intensity[a]
115 (1554.51-1568.09)	1565.4833	3.3
	1565.5074	3.3
	1565.6178	2.6
	1565.7749	2.6
114 (1567.62-1581.43)	1570.2447	2.8
	1570.2631	2.8
	1575.9826	1.7
	1576.0830	1.7
	1578.1163	2.0
	1578.3090	2.0
113 (1580.97-1595.03)	1583.0316	2.7
	1583.0354	2.7
	1584.2477	2.2
	1584.2530	2.2
	1584.8027	3.3
	1584.8095	3.3
	1586.2467	1.8
	1586.2511	1.8
	1586.9235	2.8
	1586.9379	2.8
	1589.0031	1.3
	1589.0036	1.3
	1589.6477	1.1
	1589.7165	2.2
	1589.7411	2.2
	1589.7794	1.1
	1591.4772	1.3
	1591.7072	1.3
	1593.2025	1.6
	1593.2396	1.6
112 (1594.56-1608.86)	1597.2455	3.1
	1597.2738	3.1
	1607.9701	3.2
	1607.9805	3.2
111 (1608.40-1622.96)	1619.4544	3.0
	1619.4687	3.0
110 (1622.49-1637.31)	1623.4899	3.4
	1623.5854	3.4
	1627.0010	1.3
	1627.0627	1.3
	1630.1973	1.9
	1630.2584	1.9
	1631.5279	1.7
	1631.5752	1.7
	1631.6949	2.8
	1631.7374	2.8
	1634.1470	2.5
	1634.2041	2.5

Table 4
(Continued)

Order No.	lambda (nm)	Intensity[a]
110 (1622.49-1637.31)	1635.0650	3.1
	1635.1954	3.1
	1636.0209	2.2
	1636.0562	2.2
109 (1636.85-1651.93)	1638.8244	2.9
	1638.8740	2.9
	1641.4641	2.6
	1641.4834	2.6
	1644.1965	3.2
	1644.2346	3.2
	1644.7252	2.4
	1644.7980	2.4
	1647.5648	2.7
	1647.7318	2.7
	1647.9059	2.8
	1647.9064	2.8
	1650.2244	3.3
	1650.2486	3.3
108 (1651.47-1666.83)	1655.3723	2.8
	1655.3906	2.8
	1658.5797	1.9
	1658.6848	1.9
	1660.9994	2.1
	1661.2053	2.1
107 (1666.37-1682.02)	1668.9178	2.7
	1668.9225	2.7
	1670.2604	2.2
	1670.2674	2.2
	1670.8813	3.2
	1670.8891	3.2
	1672.4707	1.8
	1672.4771	1.8
	1673.2396	2.8
	1673.2563	2.8
	1673.2965	1.2
	1673.4354	1.2
	1675.3832	1.5
	1675.5234	1.3
	1675.5256	1.3
	1675.6299	1.5
	1676.3430	2.2
	1676.3715	2.2
	1680.2152	1.6
	1680.2584	1.6
106 (1681.55-1697.49)	1684.0326	3.0
	1684.0637	3.0
	1690.3502	3.5
	1690.3857	3.5

Table 4
(Continued)

Order No.	lambda (nm)	Intensity[a]
106 (1681.55-1697.49)	1695.5012	3.1
	1695.5145	3.1
105 (1697.03-1713.27)	1707.8309	3.0
	1707.8430	3.0
	1712.3152	3.4
	1712.4166	3.4
104 (1712.80-1729.35)	1721.0109	2.8
	1721.0529	2.8
	1721.1371	1.3
	1721.1957	1.3
	1722.1701	1.1
	1722.2281	1.1
	1724.2740	1.9
	1724.3338	1.9
	1724.7926	3.1
	1724.9320	3.1
	1725.7359	1.7
	1725.7854	1.7
	1728.2584	2.4
	1728.3152	2.4
103 (1728.89-1745.76)	1730.3188	2.1
	1730.3553	2.1
	1733.0621	2.8
	1733.1117	2.8
	1735.0779	2.4
	1735.1525	2.4
	1735.9586	2.5
	1735.9787	2.5
	1738.2906	2.7
	1738.4705	2.7
	1738.6504	3.1
	1738.6887	3.1
	1742.7043	2.7
	1742.7047	2.7
	1744.9846	3.2
	1745.0088	3.2
102 (1745.29-1762.49)	1750.0682	1.9
	1750.1775	1.9
	1750.5801	2.7
	1750.5994	2.7
	1752.8254	2.2
	1753.0475	2.2
101 (1762.03-1779.56)	1764.9828	2.6
	1764.9879	2.6
	1766.0234	1.3
	1766.1695	1.3
	1766.4840	2.1
	1766.4922	2.1

Table 4
(Continued)

Order No.	lambda (nm)	Intensity[a]
101 (1762.03-1779.56)	1767.1770	3.2
	1767.1854	3.2
	1768.4160	1.5
	1768.6826	1.5
	1768.9598	1.7
	1768.9674	1.7
	1769.8352	2.7
	1769.8533	2.7
	1772.3844	1.3
	1772.3877	1.3
	1773.3299	2.2
	1773.3611	2.2
	1777.6891	1.6
	1777.7369	1.6
100 (1779.09-1796.97)	1781.1307	2.9
	1781.1643	2.9
	1788.0117	3.5
	1788.0480	3.5
	1793.4666	3.0
	1793.4822	3.0
99 (1796.51-1814.75)	1799.3619	3.5
	1799.4305	3.5
	1806.7883	3.0
	1806.7986	3.0
	1811.7965	3.3
	1811.9023	3.3
98 (1814.28-1832.89)	1821.0805	2.7
	1821.1223	2.7
	1825.3479	3.1
	1825.4949	3.1
	1828.3209	1.3
	1828.3730	1.3
	1831.3029	1.9
	1831.3586	1.9

[a] The intensity values are in arbitrary units in log scales.

Table 5

OH lines in *K*- band (Rousselot et al. 2000)

Order No.	lambda (nm)	Intensity[a]
92 (1928.11-1950.19)	1934.9914	2.6
	1935.0324	2.6
	1939.8393	3.0
	1939.9959	3.0
91 (1949.73-1971.27)	1951.8051	2.3
	1951.8828	2.3
	1952.8408	1.2
	1952.8822	1.2
	1955.5104	1.8
	1955.5590	1.8
	1956.0004	2.6
	1956.2061	2.6
	1957.2924	1.5
	1957.3514	1.5
	1959.3170	2.2
	1959.3670	2.2
	1961.8494	1.9
	1961.8953	1.9
	1964.2236	2.6
	1964.2697	2.6
	1967.7859	2.2
	1967.8137	2.2
	1969.8348	1.9
	1969.9527	1.9
	1970.1898	2.8
	1970.2268	2.8
90 (1970.80-1992.82)	1973.4920	2.1
	1973.7500	2.1
	1975.1486	2.4
	1975.1543	2.4
	1977.1744	2.9
	1977.1980	2.9
	1983.9643	2.4
	1983.9814	2.4
	1989.1355	1.3
	1989.2967	1.3
	1992.3512	1.6
89 (1992.36-2014.87)	1992.6654	1.6
	2000.4971	2.3
	2000.5059	2.3
	2000.8148	3.3
	2000.8178	3.3
	2002.4758	1.8

Table 5

(Continued)

Order No.	lambda (nm)	Intensity[a]
89 (1992.36-2014.87)	2002.4902	1.8
	2003.3158	2.9
	2003.3264	2.9
	2005.7506	1.4
	2005.7664	1.4
	2006.8877	2.4
	2006.9113	2.4
	2011.5766	2.0
	2011.6184	2.0
88 (2014.41-2037.43)	2017.4240	1.4
	2017.4889	1.4
	2019.3020	2.6
	2019.3434	2.6
	2027.5646	3.2
	2027.6033	3.2
	2033.9371	2.8
	2033.9623	2.8
87 (2036.96-2060.51)	2041.2305	3.2
	2041.3055	3.2
	2049.9357	2.7
	2049.9371	2.7
	2056.2953	3.1
	2056.4143	3.1
86 (2060.05-2084.14)	2067.2668	2.5
	2067.3021	2.5
	2072.8170	2.9
	2072.9859	2.9
85 (2083.68-2108.34)	2085.9871	2.2
	2086.0621	2.2
	2090.8451	2.5
	2091.0686	2.5
	2101.2189	1.1
	2101.2408	1.1
	2103.3090	1.6
	2103.3438	1.6
	2105.3072	1.3
	2105.3775	1.3
	2106.1498	1.8
	2106.2689	1.8
	2106.7729	2.0
	2106.8141	2.0
84 (2107.87-2133.11)	2109.6316	1.7
	2109.6889	1.7

Table 5
(Continued)

Order No.	lambda (nm)	Intensity[a]
84 (2107.87-2133.11)	2110.4275	2.1
	2110.7104	2.1
	2111.5652	2.4
	2111.6061	2.4
	2115.5926	2.0
	2115.6307	2.0
	2117.6387	2.6
	2117.6727	2.6
	2123.2354	2.2
	2123.2494	2.2
	2124.9480	2.6
	2124.9705	2.6
	2127.8219	1.3
	2127.9893	1.3
	2131.6180	1.5
	2131.9652	1.5
	2132.5914	2.2
	2132.6033	2.2
83 (2132.65-2158.50)	2150.4980	2.1
	2150.5109	2.1
	2150.7291	3.0
	2150.7326	3.0
	2152.8553	1.6
	2152.8773	1.6
	2153.7459	2.7
	2153.7586	2.7
	2156.7650	1.2
	2156.7908	1.2
82 (2158.03-2184.51)	2158.0498	2.2
	2158.0787	2.2
	2163.6973	1.8
	2163.7486	1.8
	2170.7426	1.3
	2170.8227	1.3
	2171.0932	2.4
	2171.1408	2.4
	2180.2111	2.9
	2180.2514	2.9
81 (2184.05-2211.18)	2187.3348	2.5
	2187.3689	2.5
	2195.5240	3.0
	2195.6035	3.0
	2205.2320	2.5
	2205.2412	2.5
80 (2210.71-2238.52)	2212.4875	2.9
	2212.6160	2.9
	2224.7682	2.3
	2224.7936	2.3

Table 5
(Continued)

Order No.	lambda (nm)	Intensity[a]
80 (2210.71-2238.52)	2231.1799	2.7
	2231.3650	2.7
79 (2238.05-2266.56)	2245.9926	2.1
	2246.0602	2.1
	2251.6727	2.4
	2251.9211	2.4
78 (2266.10-2295.34)	2268.9822	1.7
	2269.0982	1.7
	2274.0375	2.0
	2274.3555	2.0
	2293.8246	1.2
	2293.9947	1.2
77 (2294.87-2324.87)	2298.3535	1.5
	2298.7475	1.5
76 (2324.40-2355.19)	-	
75 (2354.72-2386.33)	-	
74 (2385.86-2418.33)	-	
73 (2417.86-2451.21)	-	
72 (2450.74-2485.02)	-	
71 (2484.55-2519.79)	-	

[a] The intensity values are in arbitrary units in log scales.

Table 6

U lines in *K*- band (Conway et al. 1984)

Order No.	lambda (nm)	Intensity [a]
92 (1928.11-1950.19)	1930.3566	5
	1931.6143	3
	1933.3101	5
	1934.2666	2
	1935.5209	2
	1935.5935	2
	1936.4132	4
	1936.4320	4
	1937.3718	2
	1938.4842	2
	1943.4616	3
	1943.8999	5
	1943.9161	5
	1944.0952	6
	1945.8603	4
	1948.1439	2
	1949.2524	3
91 (1949.73-1971.27)	1949.8085	2
	1950.3290	2
	1950.4146	5
	1954.8034	2
	1956.6691	6
	1956.7174	3
	1958.5703	5
	1959.1590	2
	1959.3506	3
	1960.5986	3
	1961.9065	4
	1962.8919	2
	1963.3316	2
	1963.5799	2
	1966.0986	3
	1967.8783	6
	1970.0653	2
	1970.3435	5
90 (1970.80-1992.82)	1971.0119	5
	1972.2295	6
	1972.6442	2
	1973.6647	4
	1975.4694	5
	1978.3446	2
	1982.1111	2
	1982.5127	2

Table 6

(Continued)

Order No.	lambda (nm)	Intensity [a]
90 (1970.80-1992.82)	1983.1629	5
	1989.1259	5
	1989.3122	6
	1990.2435	2
	1990.6935	2
	1990.7949	2
	1991.9949	2
89 (1992.36-2014.87)	1996.2542	2
	1996.8885	3
	2002.0629	3
	2002.7125	2
	2002.9142	6
	2003.3448	2
	2004.1731	2
	2004.6637	5
	2006.6730	3
	2007.0846	6
	2009.1670	5
	2009.8628	5
	2012.1259	3
88 (2014.41-2037.43)	2016.1628	5
	2018.6719	2
	2020.3547	4
	2021.4872	6
	2022.4753	4
	2024.0727	2
	2024.2239	2
	2026.6591	3
	2029.2982	6
	2029.5108	3
	2032.8016	3
	2032.8476	2
	2033.8688	4
	2034.4423	4
	2035.5787	4
	2035.7195	5
	2036.1569	2
	2036.9300	3
87 (2036.96-2060.51)	2037.0113	2
	2038.6970	3
	2039.5996	3
	2039.9125	4
	2041.4438	2

Table 6
(Continued)

Order No.	lambda (nm)	Intensity [a]
87 (2036.96-2060.51)	2043.6349	2
	2043.9106	5
	2043.9553	2
	2044.7585	6
	2045.4993	4
	2049.8050	2
	2051.3380	2
	2055.4304	5
	2057.2652	5
	2059.0872	5
	2059.2431	6
86 (2060.05-2084.14)	2062.3060	2
	2063.6538	3
	2067.0604	3
	2070.9366	6
	2071.5544	3
	2075.1245	5
	2076.3964	3
	2079.4041	2
85 (2083.68-2108.34)	2086.7373	5
	2087.1663	3
	2089.7445	4
	2090.4810	2
	2091.5702	2
	2092.6324	3
	2092.8002	2
	2096.6413	2
	2097.3981	2
	2098.7064	2
	2101.3065	6
	2106.0963	2
	2106.4383	5
84 (2107.87-2133.11)	2108.8593	5
	2112.7829	2
	2115.1344	6
	2115.2163	3
	2118.4205	2
	2125.3718	5
	2131.0747	4
	2131.9066	4
83 (2132.65-2158.50)	2136.0592	3
	2136.3769	3
	2138.2096	6
	2139.8673	5
	2140.6730	2
	2142.6885	6
	2143.0554	3
	2143.5699	3

Table 6
(Continued)

Order No.	lambda (nm)	Intensity [a]
83 (2132.65-2158.50)	2144.6571	5
	2144.8149	3
	2144.9654	2
	2145.8247	5
	2146.6611	4
	2149.8631	5
	2150.1770	2
	2151.0862	2
	2152.7974	2
	2153.1918	3
82 (2158.03-2184.51)	2159.2448	5
	2160.1071	5
	2161.1291	3
	2161.2435	3
	2163.9045	4
	2168.5581	5
	2169.9294	6
	2173.3782	2
	2175.3838	5
	2176.4301	4
	2181.7788	5
	2182.4531	2
	2183.6612	3
81 (2184.05-2211.18)	2184.9299	5
	2185.8602	2
	2185.9404	6
	2189.4716	4
	2190.5844	2
	2191.4268	5
	2191.9269	5
	2196.0922	4
	2203.3338	2
	2205.8923	2
	2206.6701	6
80 (2210.71-2238.52)	2213.2116	5
	2219.2790	3
	2224.6476	5
	2225.1307	2
	2227.7818	2
	2228.6686	5
	2230.3778	6
	2231.2270	2
	2233.2475	2
	2237.6100	4
79 (2238.05-2266.56)	2238.1884	4
	2238.2917	2
	2238.4820	4
	2239.3122	2

Table 6
(Continued)

Order No.	lambda (nm)	Intensity[a]
79 (2238.05-2266.56)	2241.7976	2
	2242.6342	5
	2245.4527	4
	2246.4908	5
	2247.0537	6
	2252.5049	5
	2258.5268	3
	2259.7537	4
	2260.1122	2
	2262.6533	3
	2264.4251	2
	2265.2530	3
78 (2266.10-2295.34)	2266.5813	3
	2277.1631	5
	2278.3252	2
	2278.4280	4
	2281.7146	6
	2287.9808	5
	2293.2697	3
77 (2294.87-2324.87)	2299.8561	6
	2304.2531	6
	2304.9239	5
	2306.1363	6
	2310.5451	6
	2312.1432	2
	2312.8719	2
	2316.8732	5
	2316.9505	2
	2317.5100	2
	2318.8460	3
76 (2324.40-2355.19)	2325.4186	2
	2326.8081	3
	2328.9899	5
	2331.4175	5
	2334.0436	2
	2338.5757	2
	2343.1128	6
	2349.2300	2
	2350.7757	4
	2353.1045	3
75 (2354.72-2386.33)	2357.7588	6
	2369.0244	5
	2369.6474	5
	2371.4181	2
	2372.2524	2
	2372.6797	5
	2374.0202	4
	2378.4550	2

Table 6
(Continued)

Order No.	lambda (nm)	Intensity[a]
75 (2354.72-2386.33)	2381.2211	4
74 (2385.86-2418.33)	2389.7289	3
	2391.7409	6
	2393.4954	3
	2394.0026	2
	2395.0197	3
	2395.1843	2
	2395.2067	3
	2396.5569	5
	2398.3496	2
	2400.2245	5
	2401.4983	3
	2402.2079	3
	2402.6991	2
	2403.8682	6
73 (2417.86-2451.21)	2418.2376	5
	2418.4487	5
	2418.8564	4
	2422.3756	2
	2423.6349	2
	2428.5544	3
	2436.2548	2
	2450.2585	5
72 (2450.74-2485.02)	2453.9558	3
	2454.5480	4
	2457.3550	4
	2459.0017	4
	2459.3149	2
	2460.4441	4
	2460.9030	2
	2467.3142	2
	2468.6147	2
	2472.2105	3
	2479.3556	2
	2481.0516	5
	2481.7757	2
	2484.0555	4
71 (2484.55-2519.79)	2486.1033	3
	2499.6881	5
	2501.4796	5
	2502.9935	6
	2504.9962	6
	2506.3417	3
	2509.9771	2
	2512.3621	3
	2513.0838	3
	2517.6620	2

[a] The intensity values are in arbitrary unit. Increment of 1 represents a factor of 3 increases in intensities.

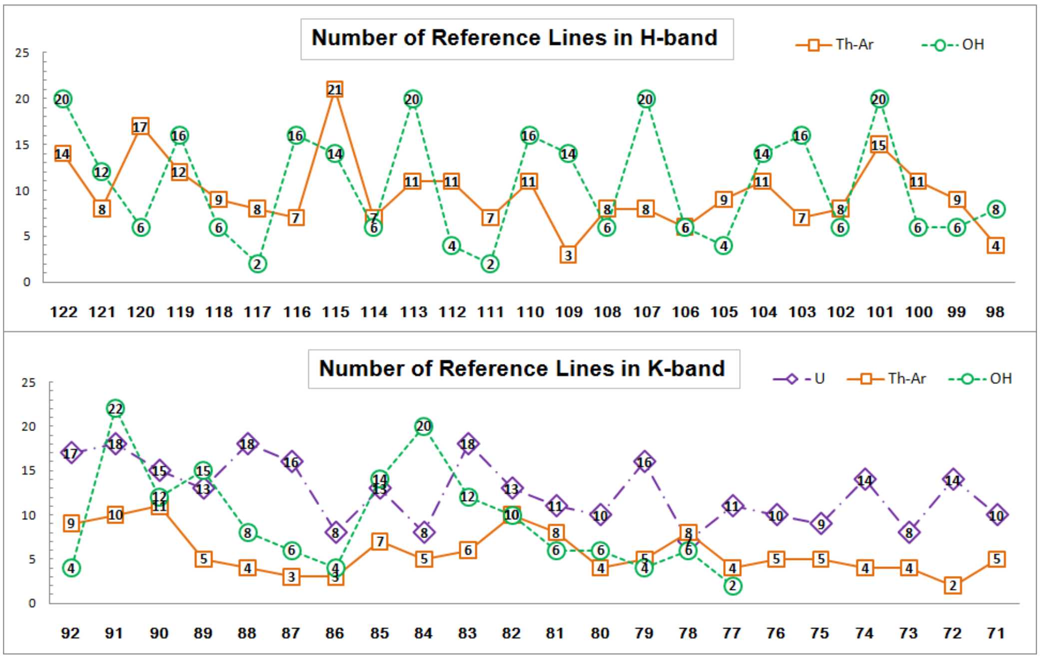

Figure 16. Histogram shows number of lines at each *H*- and *K*- band order. Green circles represent the OH emission liens, orange squares are Th-Ar line and Purple diamonds show the number of uranium lines. The number of uranium lines at *H*- band are not shown.

4. FLAT SOURCE

To correct pixel-to-pixel sensitivity variations of detectors, we need to take flat frames. Flat frames also provide solutions to extract the echelle order stripes from the row spectrum and correct the intensity uniformity which caused by the intrinsic property of spectrograph optics.

The purpose of designing the flat source is to get uniform illumination at the IGRINS entrance slit using blackbody source. We will use tungsten halogen lamp with integrating sphere to make blackbody source. Integrating sphere need to be coated with gold which performs high reflectivity in infrared wavelength.

Figure 17 shows the performance of the integrating sphere and the Labsphere infragold model. The throughput of integrating sphere is the ratio of the total flux out to the total flux in. This value is determined by the sphere's reflectance, diameter, and number of ports. The throughput at the output port τ is given in following equation:

$$\tau = \frac{\phi_e}{\phi_{in}} = \frac{\rho A_e / A_s}{\left(1 - \rho\left(1 - A_p / A_s\right)\right)}$$

ϕ_e represents total flux exiting port and ϕ_i is total incident flux. A_e and A_s are area of exit port and surface area of sphere respectively. A_p is a sum of all port areas and ρ is sphere wall reflectance ($0 \leq \rho \leq 1$). We are considering to choose 3inch diameter sphere and the reflectance of gold is 0.95.

The flat source from the integrating sphere output port will pass through the calibration optics simulating the same f-ratio with the telescope and will be illuminated as an extended source at IGRINS entrance slit.

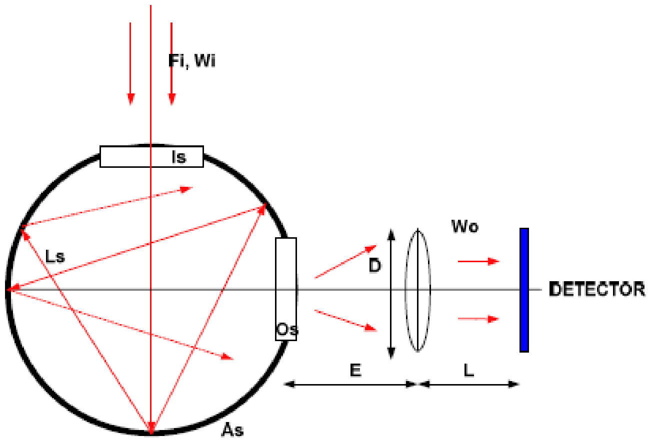

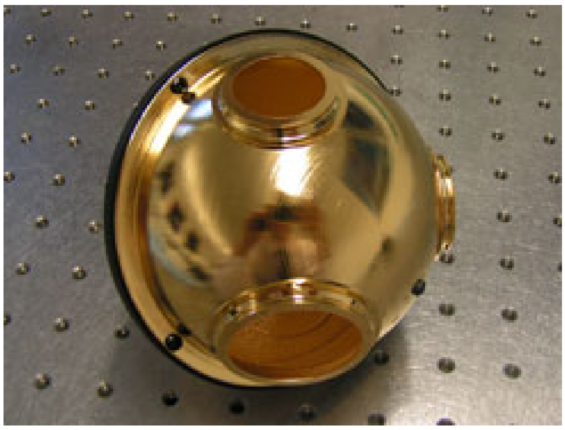

Figure 17. The performance of integrating sphere and gold-coated integrating sphere (Labsphere). We put the illumination of tungsten halogen lamp into integration sphere and we get uniform output source.

5. OPTO-MECHANICAL DESIGN

5.1 Optical Design

5.1.1 Concept

In general, the spectroscopic system requires an independent optical system for the calibration unit. The resultant beam of the calibration optics goes through the dewar window and illuminate on the slit. There are two main purposes of calibration optics. One is to provide a beam that simulates with the telescope beam. The f-ratio of beams from the calibration optics and the telescope optics should be same. The other purpose is to make the extended calibration source to uniformly illuminate the focal plane (Bortoletto et al. 2005).

We have considered two reference designs, one is Subaru Nasmyth calibration unit and another is BOES (Bohyunsan Optical Echelle Spectrograph) calibration design. With two kinds of calibration source, line emitting lamp and flat source, our original plan was to place both sources in an integrating sphere. In this case, the calibration optics alignment will be similar to Subaru calibration unit (See Figure 18). But we recognized that we cannot put the line emitting lamp in the integrating sphere. If we use diffused beam of the line lamp passed though integrating sphere, we need long exposure time compare to tungsten lamp because of it is originally not very bright and its relatively large size (150 mm × 40 mm) is also problem. Therefore two sources need to be illuminated into calibration optics separately. We can follow BOES design in this case.

IGRINS has several different designs of input relay optics for different telescopes. The f-ratios of candidates are between f/8 and f/16 and each input relay optics has an optimized cold stop. But the position of telescope focal plane from the IGRINS dewar will be kept the same for the candidate telescopes. Therefore, the f-ratio of input beam is the only issue when we need to synchronize the calibration optics with the telescopes.

To simulate the telescope beam, the exit pupil position of calibration unit should be located on the exit pupil position of the telescope. Thus the relay lens of calibration unit should be replaced when the telescope is changed. In this situation, we can think one alternative solution that is to make the calibration optics with the fastest f-ratio and we only replace the stop when the telescope is changing. One problem caused in this case is we lose some part of light from calibration sources by different size of the stop which will be optimized to the changed telescope. But the light loss can be compensated by increased brightness of the calibration sources and increased exposure time. Even if we need to replace the calibration sources with higher-watt lamps, the cost and time-wasting should be much lower than making an every different optics and repeating alignment for each telescope.

5.1.2 Requirement

To determine the requirement for calibration optics, we assume the fastest f-ratio is f/8 and the slowest f-ratio is f/16. We describe the requirements we adjusted to the design process below.

Since IGRINS contains the input optics in the dewar before reach the entrance slit, the beam from calibration optics will pass through this input optics and will have f/10 after input optics (Fig 5. in Section 2). The actual size of slit length is 1.94 mm that represents 10″ at sky for 4m telescope and we determined that our calibration image needs to have ~3mm on the slit to have the spare illumination area around slit. The focus of our calibration system is the same location with the telescope focal plane, which is located 40.35 mm before IGRINS dewar window. At this focus, the parameter 3 mm at the slit represents 2.6 mm so our calibration optics will have 2.6 mm image size. The calibration source size will be limited by the hallow cathode lamp (~5mm) because the commercial Th-Ar or uranium lamps have industrial standard size.

Another important issue is flatness of photon flux. Ideally, to take a flat frame for flat-fielding, the illuminated beam should have perfectly uniform distribution at entrance slit. Thus we limited the allowable error of photon flux from the calibration source to be less than 1% after the calibration optics.

The total length of the optical design is limited by the 380 × 660mm calibration box (Figure 19). Since the IGRINS dewar has already designed and also the window location is fixed, calibration box cannot be protruded out over the IGRINS dewar because of the balancing problem. We estimated the space in the calibration box and determined that suitable total length of calibration optics is ~550mm.

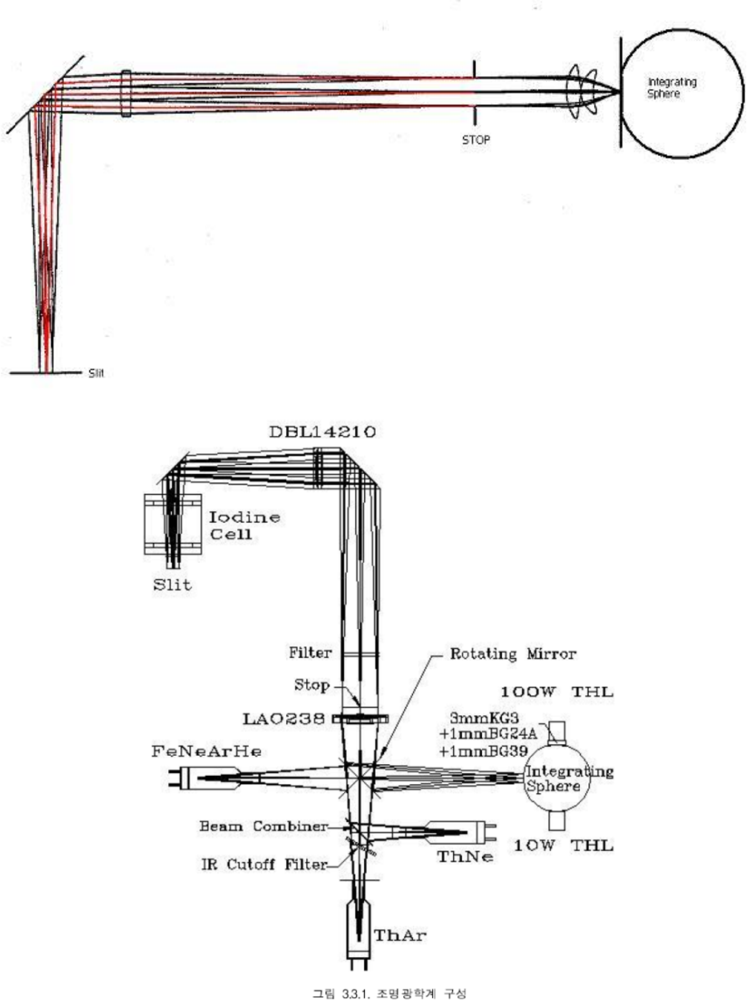

Figure 18. An optical design of Subaru Nasmyth calibration unit (top) and BOES calibration optics (bottom).

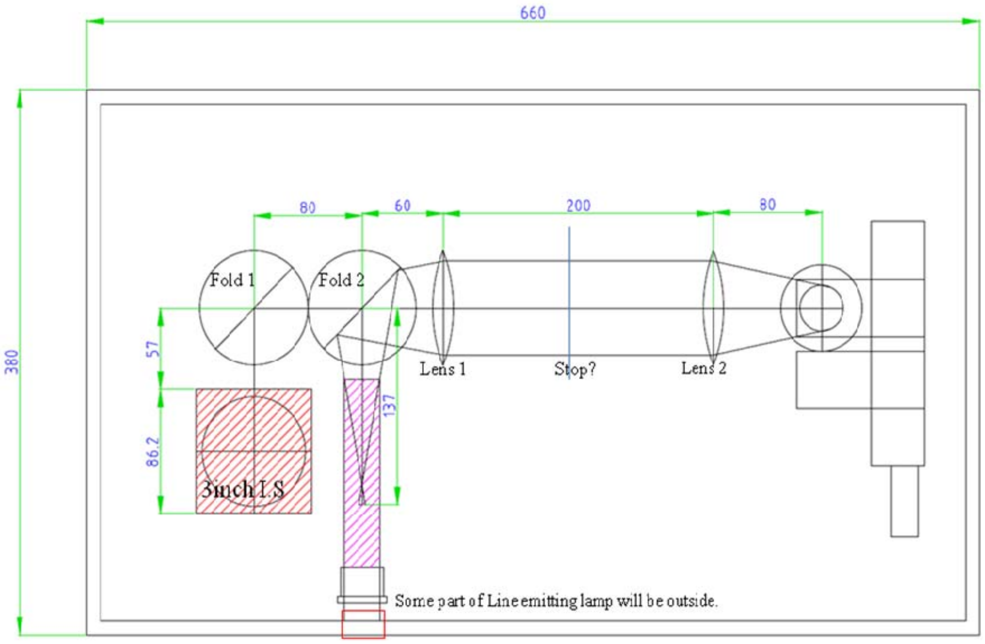

Figure 19. Space estimation for calibration optics. The total length of optics is limited by calibration box space and window location at IGRINS dewar wall.

5.1.3 Optics Design and Performance

In this section, we introduce our calibration optics design. As shown in Figure 20, we optimized two optical designs which correspond to required fastest f-ratio (f/8) and slowest f-ratio (f/16). Two optical systems are designed exactly identical but the stop sizes are different only.

Our optics consists of two groups of lenses (see Figure 20 and Table 7). We call them group 1 and group 2 respectively and each group contains two lenses. They are lens 1-1, 1-2, and lens 2-1, 2-2. All the lenses have spherical curvatures for both sides symmetrically but only lens 1-1 has different curvature for each side. Lens 1-1, 1-2, and 2-2 are designed with CaF_2 material and lens 2-1 is S-FTM 16. The indexes of refraction are 1.424 and 1.561 for CaF_2 and S-FTM 16 respectively. The sizes of lenses are 80 mm diameter for group 1 and 30 mm for group 2. The source size is defined as 5m because our line lamp source has commercial standard and the image size at the focal plane satisfied the value of 2.6mm.

To optimize our design according to flux flatness requirements, we conducted LightTools analysis. The calibration optics is illumination system, not an image-forming system because it uses extended source and illuminate the final image with a required size and flatness at the slit. To conduct the LightTools analysis, we need to set the basic conditions. We apply the Code V data of calibration optics to LightTools and we define a source size and divergence angle. We set the 5mm source size and 7˚ divergence angle for upper and down sides. Then Light Tools automatically produces 3-dimensional optic system for simulation. To check uniformity, we measure the flux flatness at the focal plane with given mashed bins. According to IGRINS optical design, pixel size at the calibration focal plane corresponds to 33.7 μm. Considering 3.7 pixel sampling of IGRINS, the required mashed bin number is 21 x 21 at focal plane. Light Tools scatter the photons into the lens system using Monte-Carlo method and measure the photon flux flatness for the direction of x and y at the focal plane. The flatness error value is 0.92% for the f/8 calibration optics and 0.76% for the f/16 optics (Figure 21).

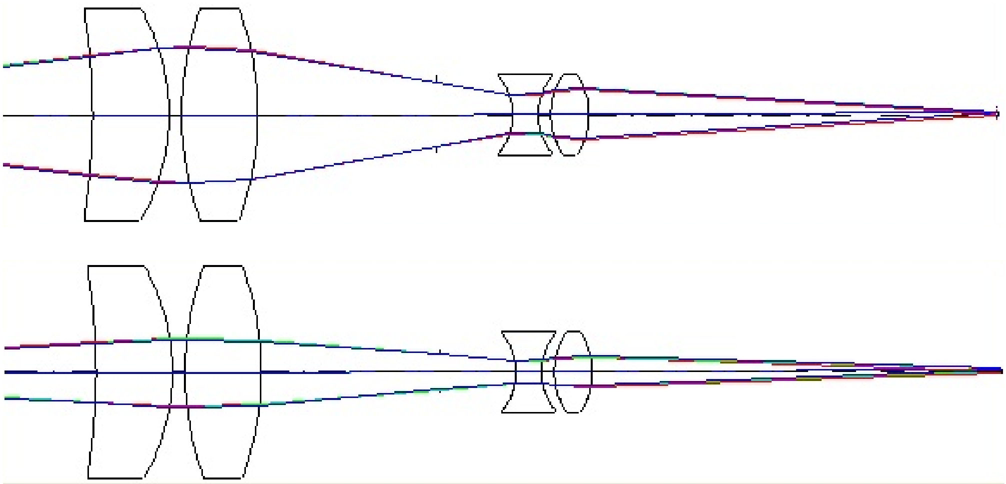

Figure 20. IGRINS calibration optics design layout. Optic designs are simulate f/8 (top) and f/16 telescope beam (bottom).

Table 7

Calibration optics parameters.

		Radius	Thickness	Material	Index @1.97μm	Semi aperture	
						F/8 optic	F/ 16 optic
Group 1	Lens 1-1	-250	30	CaF_2	1.424	23.9	12.2
		-85	5	Air		26.8	13.8
	Lens 1-2	120	30	CaF_2	1.424	27.0	13.8
		120	70	Air		25.6	13.0
Stop			30	Air		12.6	6.8
Group 2	Lens 2-1	-23.38	10	S-FTM16	1.561	7.9	4.5
		23.38	5	Air		8.3	4.8
	Lens 2-2	28.84	15	CaF_2	1.424	9.8	5.6
		-28.84	160	Air		10.6	6.2

Total length 560mm. EFL- 141.2mm

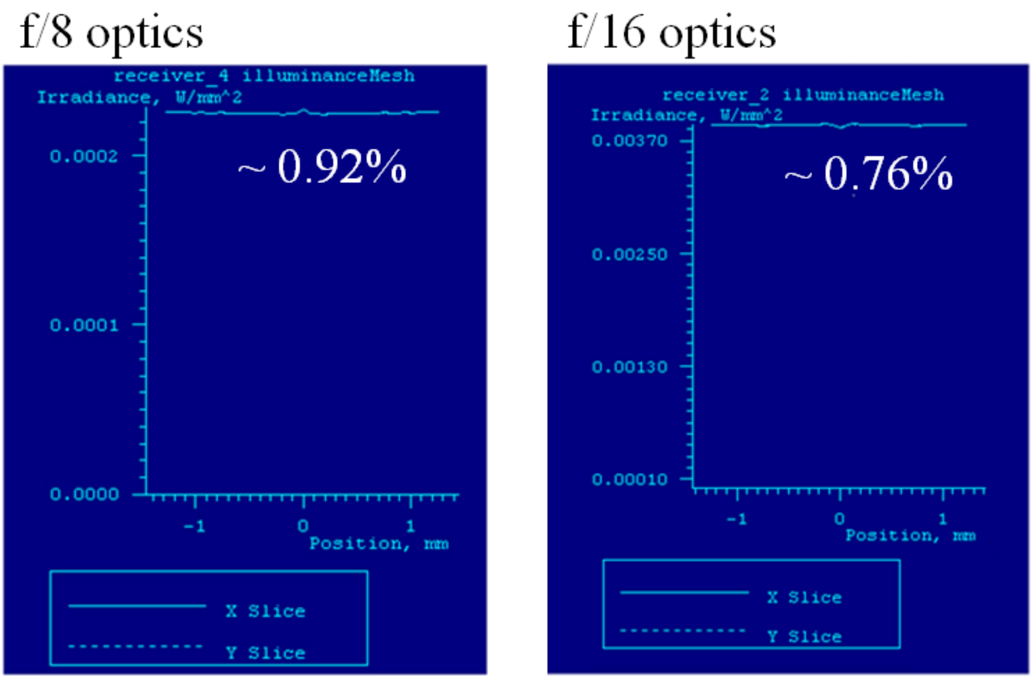

Figure 21. Flatness error of photon flux at focal plane (2.6mm ×2.6mm). The value is 0.92% for f/8 optics and 0.76% for f/16 optics. (Light Tools analysis).

5.2 Lens Barrel

Calibration lens barrel will have the same concepts with the IGRINS *H*- and *K*- Band camera barrel. Even the IGRINS camera barrels are design for cold optics and calibration lens are warm optics, we will have a same strategy for the unity of instrument design and for the safety.

The camera barrel of IGRINS aims to have the IfA (Institute for Astronomy, Hawaii University) lens barrel design as a reference. IfA group designed instruments operating at IRTF (NASA Infrared Telescope Facility), which are CSHELL (Greene et al. 1993), NSFCAM (Shure et al. 1994), NSFCAM2, and SpeX (Rayner et al. 2002). One of the main speciality of IfA barrel design is to have three axial hard points and an axial spring for each lens. And there is two radial hard points for one lens and one radial spring which will fix another third radial point.

Here are several key points in designing of the the multiple lens cell from Vern stahlberger (IfA). Remember these issues are pointed for the cold optics and our calibration system following this strategy even warm optics.

- Axial defining points and lens spacers tangentially beveled to fit lens-curvature at point of contact.
- Radial defining points heights adjusted so lenses are centered when cold.
- Spring forces about 3 times lens weight
- Lens spacer diameters must be same size as lens when cold.
- Radial springs should not dig into lens.

One issue in calibration barrel is the stop changing. Due to the plan that IGRINS will be replaced to other telescopes in the future, we need to be easily accessible to stop. Therefore, we determined to have the barrel design of two separable pieces (Figure 22). In Figure 22, we showed disassembled calibration lens barrel. Barrel 1 contains two lenses those in lens group 1 in Section 5.1.3 and three spacers. One axial spring will applied before first spacer and the radial spring will holds all the lenses and spacers. In barrel 2, the stop is mounted with the radial spring and the axial spring and two lenses in lens group 2 are mounted from the opposite direction where the stop is inserted. These two lenses also mounted with three spacers and one radial spring, and axial spring. The bottom image of Figure 23 is showing how three axial points and two radial points are located in lens barrel.

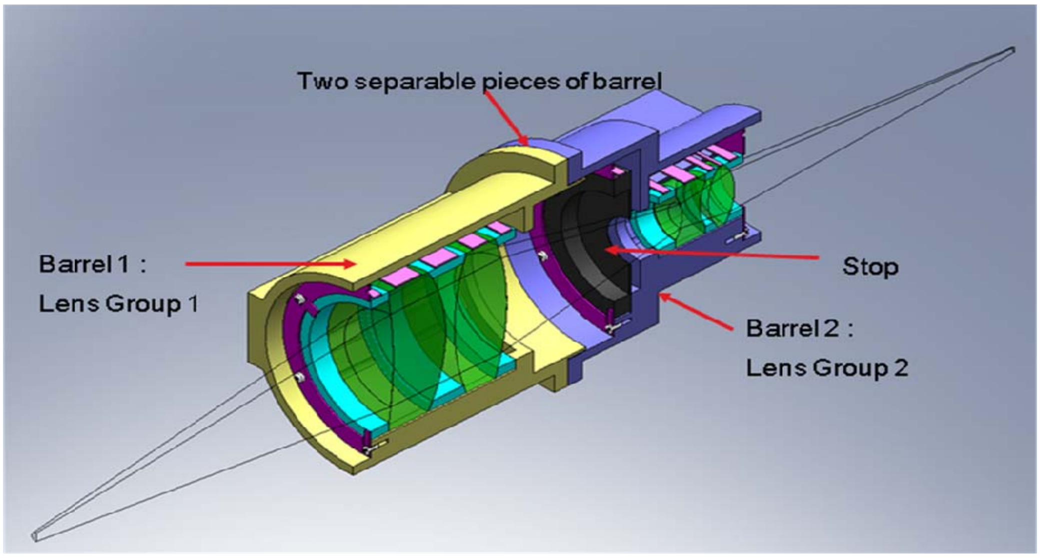

Figure 22. Calibration optics lens barrel. Barrel is separable into two pieces to easily access for when we change the stop.

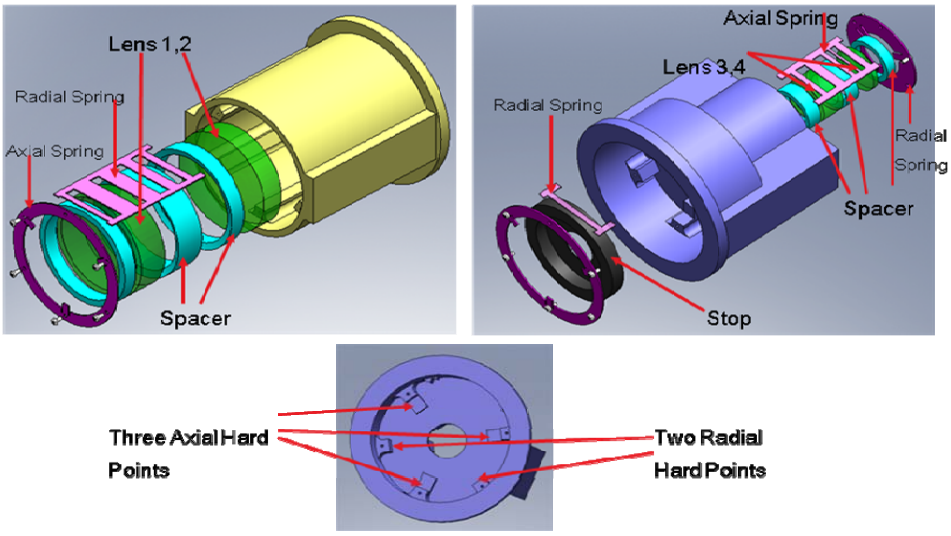

Figure 23. Compositions of barrel 1(left) and barrel 2(right). Each barrel contains the axial spring and radial spring. The bottom figure shows three axial hard points and two radial hard points of barrel.

5.3 Calibration Box Design

Figure 24 shows the designed conceptual model of the IGRINS calibration box. The bright blue colored square is the bottom plate of calibration box. The plate will be attached on the IGRINS dewar wall where the entrance window is located. There is a hole on the bottom plate which provides the path for the beam from the telescope to the IGRINS window. This hole is also for the path of the beam from calibration source when they are in use.

Beside the path hole, there is a linear stage which provides three position (see details in Section 5.4). This stage holds 45° folding mirror toward the direction of IGRINS window and one flat mirror parallel to bottom plate.

The box also contains two calibration sources, an integrating sphere for the flat-fielding and line source lamp for the line calibration. The integrating sphere and line lamp will share one movable 45° folding mirror to reflect their beam to calibration optics. A linear moving stage is holding the mirror and those three elements: integrating sphere, line lamp, folding mirror consist a *calibration lamp module*. After passing through the optics, the beam will be reflected again by 45° folding mirror toward the direction of IGRINS window.

The calibration optics lens barrel is located between the calibration lamp module and the hole for the beam path. All the elements in calibration box will mounted on the bottom plate and they will be easily accessible by removing a box top cover only.

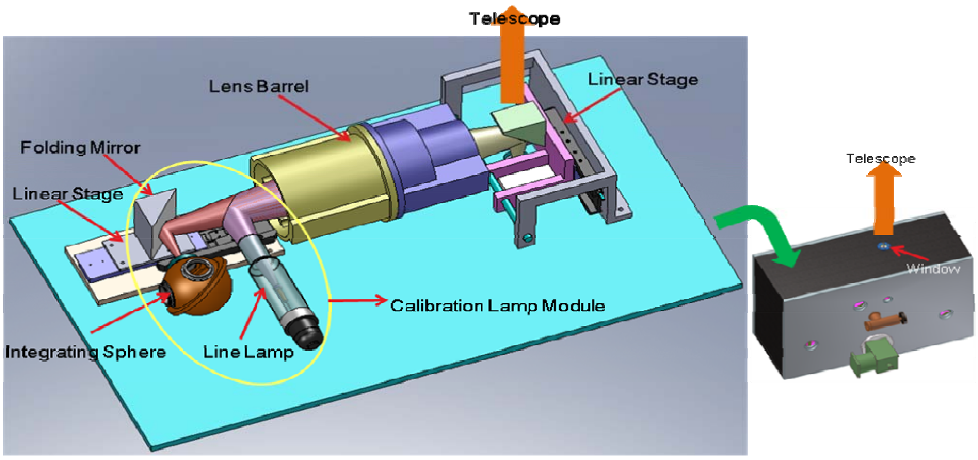

Figure 24. Conceptual model of calibration box. The system consists of integrating sphere (flat source) and line source lamp, lens barrel, folding mirror, and two linear stages. The calibration box will be attached on the dewar wall which is toward the telescope direction.

5.4 Observing Mode and Moving Part

In Figure 25, a flow chart shows a observing scenario of IGRINS. The observation starts at parking position (or a pseudo dark observing mode) and we take flat, line lamp frames, standard star or sky frames, and target frames. After the target exposure, the observer goes back to any mode due to observing situations. In the mechanical point of view, we will have 4 different observing positions according to the sources that we need to detect after all the spectrograph optics. For each modes, the source we need to look at are : (1)window cover mirror, (2)blackbody source, (3)line lamp, and (4)telescope beam.

To provide 4 different positions, the IGRINS calibration box has two moving parts. One is the observation mode changer in front of the dewar entrance window (see Figure 24) and the other is the calibration lamp selector in the calibration lamp module. Table 8 and Figure 26 shows the position options provided by two selectors.

The observation mode selector, which consists of one flat mirror, one 45^0 pick-off mirror and one blank position are set on the linear moving stage, has tree position options. When the IGRINS window is covered with a flat mirror, we call this position OD (Observation – Dark). We use this position as a parking position of IGRINS and also we can take pseudo dark in case we need it. At the position OC (Observation – Calibration), the 45^0 pick-off mirror is placed in front of the window and this mirror pick the beam from line lamp or integrating sphere and send it to the IGRINS window. At the position OS (Observation – Sky), entrance widow is clearly opened so that the telescope beam can pass through into the IGRINS dewar. We can observe celestial objects or sky frame at this mode.

By a calibration lamp selector, the second moving part, the position OC is divided into two different positions. We use one more 45^0 pick-off mirror with a linear stage in this selector. When the mirror is located at a position OC – B (observation – Calibration –Blackbody), the beam from the integrating sphere output port is picked up and is sent to lens barrel (Figure 24). At the position OC – L (observation – Calibration – Line lamp), the mirror reflect the beam from the line source lamp. Those beams from both integrating sphere and line lamp will pass through the calibration optics and reach to window pick-off mirror.

The linear stages will have position encoders themselves and we are considering to have additional sensors for the absolute position control to guarantee a repeatability of moving mechanisms.

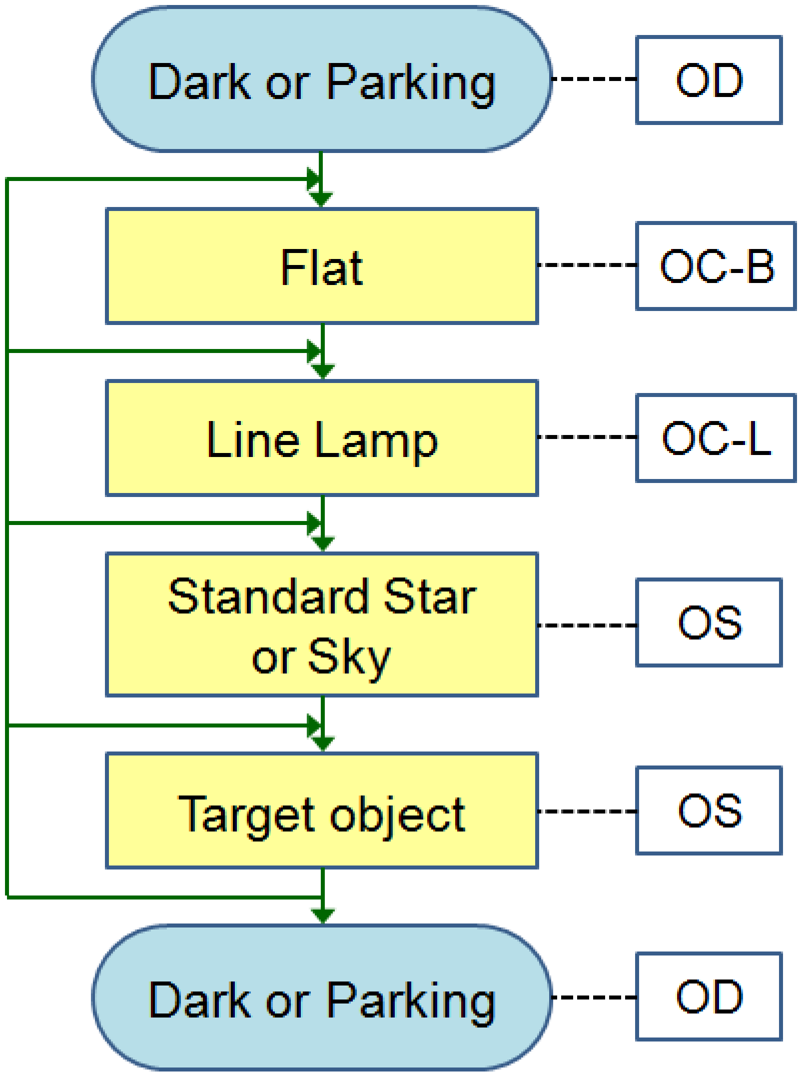

Figure 25. IGRINS observing Scenario. For each different observing mode, the moving position in calibration box is commented right side.

Table 8

Position options of moving mirrors in IGRINS calibration box.

Observation Mode Selector	**Calibration Lamp Selector**	**Purpose**
OD	-	Pseudo dark frame or parking position
OC	OC – B	Flat source observation
	OC – L	Line calibration source observation
OS	-	Celestial object or sky observations

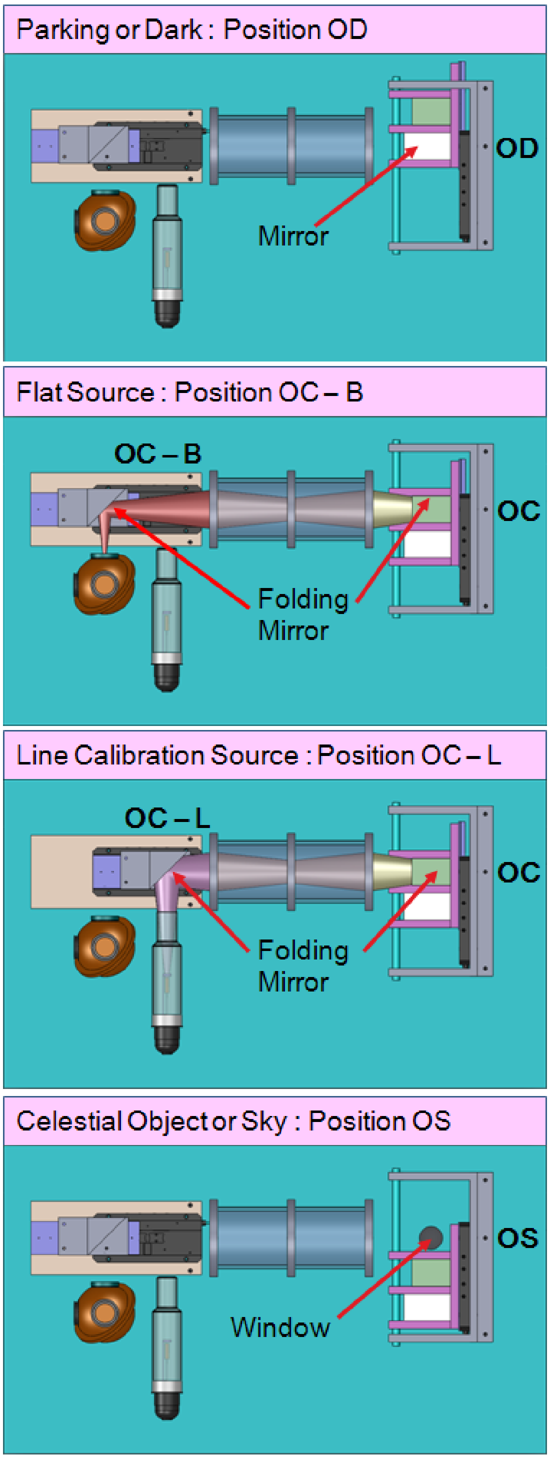

Figure 26. 4 different positions of calibration moving parts.

6. SUMMARY AND FUTURE WORK

IGRINS is a high resolution near-IR spectrograph using an immersion grating and is observing *H*- (1.49μm -1.80μm) and *K*- (1.96 μm -2.46 μm) band with a resolving power of 40,000. We aimed to design a well based calibration system for our high resolution instrument. We established the calibration concept and data reduction sequence for IGRINS. Using flat frames, line lamp frames and standard star frames, we can get order extract solution, distortion solution, wavelength solution and flux calibration.

For the selection of line reference source, we listed the details of telluric OH emissions, telluric absorption liens and hallow cathode lamps. We plotted the histograms that show the number of OH emissions, Th-Ar and U lines in *H*- and *K*- band and also the histograms showing the lines in each order. In the range of 2.3 – 2.5 μm of the *K*- band, U lamp has 8 - 14 lines while the Th-Ar and OH lines significantly decrease. We determined that U lamp is the the most preferable for our wavelength reference source. For the flat source, we use the 3 inch diameter infragold (Labsphere) integrating sphere and tungsten halogen lamp to provide a uniform near-IR blackbody radiation.

Optics was designed simulating the telescope beam of f/8 and f/16. The designs are exactly same for both optics and they are consist of two groups of lenses. The stop sizes are different only having 12.6mm and 6.8mm semi aperture. We conducted Light Tools simulation and we confirmed the flux flatness errors of images at a focal plane are 0.92% for f/8 optics and 0.76% for f/16 optics. We designed calibration box conceptual structure containing an integrating sphere, line lamp, two folding mirror, and lens barrel. Lens barrel is separable for the purpose of stop changing in the future and the lens mounting concepts are following those of IfA (Institute for Astronomy, Hawaii University). There are two moving parts in calibration box: 1) observing mode selector, 2) calibration source selector. We organized 4 positions made up by two moving parts according to IGRINS observing scenario, those are OD, OC (OC-B, OC-L) and OS.

For the detailed design in the future, we will determine actual size of the parts, i.e., linear stages, folding mirrors and will select the models. To secure the space for the calibration box between the telescope and IGRINS dewar, we need to consider the interference with telescope interface structure. Gas absorption cell for precision RV observations will be studied and the space for this gas cell will be considered in the calibration box. We also need to conduct the sensitivity simulation of the blackbody source and line lamp source with designed optics.

REFERENCES

Bean, J. L., Seifahrt, A., Hartman, H., Nilsson, H., Wiedemann, G., Reiners, A., Dreizler, S., & Henry, T. J. 2010, ApJ, 713, 210

Birney, D.S., Gonzalez, G.G., and Oesper, D. 2006, Observational Astronomy, Cambridge, Cambridge University Press, 216-229

Bortoletto, F., Magrin, D., Bonoli, C., & D'Alessandro, M. 2002, Proc. SPIE, 5897, 148

Conway, J. G., Worden, E. F., Brault, J. W., Hubbard, R. P., & Wagner, J. J. 1984, Atomic Data and Nuclear Data Tables (ADNDT), 31, 299

de Graauw, T. et al. 1998, SPIE, 3357, 336

de Graauw, T. et al. 2008, Proc. SPIE, 7010, 701004

Engleman, J. R., Hinkle, K. H., & Wallace, L. 2003, Journal of Quantitative Spectroscopy and Radiative Transfer (JQSR), 78, 1, 1

Glass, I. S. 1999, Handbook of Infrared Astronomy, Cambridge, Cambridge University Press

Greene, T.P., Tokunaga, A.T., Toomey, D.W., and Carr, J.B. 1993, Proc. SPIE, 1946, 313

Houck, J. R. et al. 2004, ApJS, 154, 18

Jaffe, D. T., Mar, D. J., Warren, D., & Segura, P. R. 2006, Proc. SPIE, 6269, 62694I

Jaffe, D. T., Wang, W., Marsh, J. P., Deen, C. P., Kelly, D., & Greene, T. P. 2008, Proc. SPIE, 7010, 70103L

Jaffe, D. T. et al. 2009, IGRINS PDR document

Jakobsen, P. et al. 2010, BAAS, 42, 396

Kaufl, H. U. et al. 2004, SPIE, 5492,1218K

Kerber, F., G. Nave, G., & Sansonetti, C. J. 2008, ApJS, 178, 374

Kim, K-. M. 2002, BOES final report

Kim, K-. M. et al, 2007, PASP, 119, 1052K

McLean, I.S., Steidel, C.C., Matthews, K., Epps, H. & Adkins, S.M. 2008, Proc. SPIE, 7014, 70142Z

Olivia, E., & Origlia, L. 1992, A&A, 254, 466

Pak, S. 2000, PKAS, 15S, 127

Pak, S. 2007, Proc. Astronomical Instrumentation, Korea, 1, 101

Palmer, B. A., Keller, R. A., & Engleman, J. R. 1980, Los Alamos National Laboratory Report (LANLr), LA-8251-MS

Rayner, J. T., Toomey, D. W., Onaka, P. M., Denault, A. J., Stahlberger, W. E., Vacca, W. D., Cushing, M. C., & Wang, S. 2002, PASP, 115, 805, 362

Rousselot, P., Lidman, C., Moreels, G., & Monnet, G. 2000, A&A, 354, 1134

Seo, H. et al. 2010, in preparation

Shure, M.A., Toomey, D.W., Rayner, J.T., Onaka, P.M., and Denault, A.J. 1994, Proc. SPIE, 2198, 614

Tokunaga, A. T. et al. 1998, Proc. SPIE 3354, 512

Vacca, W. D., Cushing, M. C., & Rayner, J. T. 2003, PASP, 115, 389

Yuk et al. 2010, Proc. SPIE, Submitted